POLITECNICO DI MILANO

Scuola di Ingegneria Industriale e dell'Informazione
Mathematical Engineering

Charge scheduling for a fleet of electric buses considering Vehicle-to-Grid technologies

Supervisors

Prof. Ola JABALI
Prof. Aurélien FROGER (Université de Bordeaux)

Candidate

Laura CODAZZI

920457

Academic Year 2020 – 2021

Alla dolce Beuzz

Contents

List of Figures

List of Tables

Sommario

Il cambiamento climatico ha reso la transizione verso la sostenibilità un processo necessario. Il settore dei trasporti è profondamente coinvolto in tale transizione in quanto è uno dei maggiori responsabili dell'inquinamento atmosferico. Nel contesto urbano, i sistemi di trasporto pubblico stanno convertendo le loro flotte in elettriche. In questo scenario è assolutamente necessaria una corretta pianificazione per ricaricare i veicoli per garantire il corretto funzionamento del servizio. Tale piano e' inoltre indespensabile affinchè i costi dell'energia e quelli per la potenza richiesta alla rete siano ottimizzati. Allo stesso tempo, un corretto processo di ricarica può aiutare a rallentare il deterioramento delle batterie. Tramite nuove tecnologie chiamate Vehicle-to-Grid, i veicoli elettrici sono in grado di restituire energia alla rete scaricando parzialmente la loro batteria. Queste tecnologie possono risultare vantaggiose per la gestione della flotta. In questo lavoro viene sviluppata una formulazione MILP per pianificare il piano di ricarica di una flotta di autobus elettrici. Il modello tiene conto dei costi dell'energia, della potenza massima richiesta alla rete e cerca di quantificare anche un costo causato dal deterioramento delle batterie. Inoltre, le sopracitate tecnologie Vehicle-to-Grid sono integrate nel contesto. Il modello si basa sul sistema di trasporto pubblico della città di Milano. Vengono modellizzate anche delle istanze di test basate su di esso. Viene quindi proposta una strategia per la risoluzione del problema e questa è anche applicata su un insieme di istanze basate sulle reali condizioni operative a Milano. Vengono poi eseguiti alcuni esperimenti per convalidare sia modello che l'euristica. Infine, attraverso un'analisi di sensibilità è indagato l'impatto delle tecnologie V2G sulla flotta.

Parole chiave: autobus elettrici, V2G, mezzi di trasporto pubblico strategie di ricarica, trasporti sostenibili, deterioramento delle batterie, logistica urbana

Abstract

The current climate condition has made a transition towards sustainability necessary. The transport sector is deeply involved in such a transition as it is responsible for a significant portion of air pollution.

In urban environments, public transportation systems are converting their fleets into electrical ones. In this scenario an optimised charging schedule is absolutely necessary to ensure the proper operation of the fleet. Furthermore, coordination is necessary to keep the cost for withdrawing energy low while avoiding the overloading of the grid. At the same time, a proper charging schedule may slow the degradation of batteries. Furthermore, bidirectional flow of the current can be achieved thanks to Vehicle-to-Grid (V2G) technologies. Such technologies are thought to be beneficial for the operations of the fleet.

In this work a MILP formulation for the charge scheduling of a fleet of electric buses is developed. The model takes into account the costs of energy, the maximum power requested from the grid and the degradation of batteries. Furthermore, V2G technologies are explicitly modelled. A matheuristic is then proposed for the efficiently solving the resulting problem. A set of instances based on the real operational conditions in Milan is proposed. Extensive experiments are performed to validate the model and the heuristic. Finally, a sensitivity analysis investigating the impact of V2Gs over a variety of setting is performed.

Keywords: electric buses, V2G, public transportation, charge scheduling, green transportation, battery degradation, city logistics

Chapter 1

Introduction

It is now common knowledge that air pollution plays a key role in damaging the ecosystem and human health. Indeed, right after climate change, air pollution is considered the second most important environmental concern for Europeans (EEA, 2020a). Despite the increasing efforts in cleaning Europe's air, improvements in air pollution are not yet satisfactory. A special attention is devoted to the level of particulate matter (PM), ammonia (NH_3) and nitrogen oxides (NO_X). Their concentration is higher in cities, where they are typically above the standard levels set in the World Health Organization's guidelines for clean air. The majority of EU Member States are currently implementing measures aimed at drastically reducing emissions by 2030 (EEA, 2020b). Sectors addressed as principal responsibles for air pollution are agriculture, energy production and transportation. In the European contest, emissions due to domestic navigation and railway transportation have decreased since 1990 (E. EEA, 2019). The same trend does not apply for road transport, international maritime transport nor aviation. However, emissions due to road transports, which constitute the highest proportion over the total (71% in 2018), are expected to decrease in the next years. Indeed, one of the major initiatives regards the structural change of the transportation sector, mainly in urban context. Road traffic is also considered the principal contributor to noise pollution, which is a growing environmental concern and has severe impacts on health conditions and other important aspects of life, such as cognitive impairment on children (EEA, 2021).

Switching to electric vehicles (EVs) seems to address the above-mentioned problems, as they are well known to reduce noise pollution and the greenhouse gases (GHG) emissions. Especially, local CO_2 emissions are almost 10 times lower compared to vehicles with internal combustion engines (Teixeira and Sodré, 2018). Furthermore, given the target of zero emissions established in the European Green Deal, the reduction of CO_2 emission will also interest the production of the energy to charge the fleet (EEA, 2020c). Despite their advantages, EVs are not widely employed. For instance, the percentage of private electric cars, even if increasing, in 2019 represented only the 3% of the total vehicles. The main causes are the high initial investments required for these fleets and logistic challenges which arise with their operation. However, batteries costs are estimated to decrease of 18% within 10 years (Schmidt et al., 2017, Finance, 2020) as well as their associated costs, like maintenance and storage. On the other hand, many studies are evaluating the

best operating conditions to properly adopt an electric fleet. Furthermore, with their progressive usage, the required facilities, as for instance charging stations, are increasing.

The public transportation sector is part of this epochal change. For instance, the public transportation system of the city of Milan (ATM) is transitioning to having a fleet of fully electric buses (EB) by 2030 (ATMWebsite, n.d.). Such a scenario will be taken into account in this work, with a focus on the charging process of the fleet. Apart from the required equipment for charging, the process itself can be really slow. This could make EVs appear less powerful than ICEs. However, in urban context EVs are showed to be more efficient (Brito et al., 2013). Special equipment, such as fast chargers, are able to speed up the charging process. Unfortunately, they are more expensive than the slow chargers, therefore there are usually few of them. Furthermore, these efficient technologies require a very high power, which may lead to an excessive load of the grid.

Another important aspect is the lifetime of the batteries. Due to the high replacement price, the investment in batteries is pivotal in the operational costs of the fleet. In some cases then, like for the mostly used Lithium-Ione batteries (LIB), there are other issues, like the environmental costs for their disposal and uncertainties with respect to Lithium itself. Even though these aspects are being investigated and efficient recycling process for LIBs are being developed (Ziemann et al., 2018), preservation of batteries themselves cannot be ignored while charging the fleet.

Lastly, costs incurred when charging the fleet may be subjected to great variability. This is due to the energy plans, whose costs for kWhs typically fluctuates during the day. In particular, industrial energy contracts usually stipulate a fee related with the maximum power retrieved from the grid, adding uncertainty to the total costs.

Vehicle-to-Grid (V2G) technologies enable EVs to support bidirectional flow of current. EVs provided with such technologies (EV-V2Gs) are able to return energy to the grid with a partial discharge of their battery. Thus, EV-V2Gs can also serve as a source of energy storage. EV-V2Gs can also decrease the operational costs. As prices of energy vary during the day, energy bought during cheaper periods can be discharged to other EVs in a high cost period. Nevertheless, since less power is retrieved from the grid, an efficient usage of V2G technologies could reduce the maximum charging power required in the planning period.

To properly address all these operational aspects, it is necessary to plan ahead the charging process. In literature these types of problems are called Charge Scheduling Problems. This class of problems is very wide. It can include different types of electric vehicles, like shared vehicles, electric freight (EFVs), EBs. Thus, the specific assumptions used in charge scheduling problems depend to the specific assumption of the context. This work inherits the assumptions of the charging scheduling problem for a fleet of EFVs in Pelletier et al., 2018, adapts them in the context of EBs of a public transportation. The contributions of this thesis are as follows.

1. We propose an enhanced Mixed integer linear program (MILP) formulation for the charge scheduling problem of Pelletier et al., 2018.

2. We introduce V2G technologies in the context of the charge scheduling problem associated to EBs.

3. We propose an effective matheuristic for the resulting problem.

4. We generate a set of test instances based on the real operational conditions in Milan.

5. We demonstrate the effectiveness of our models and heuristic on a broad set of experiments. Furthermore, we analyse the sensitivity of various problem features through a comprehensive set of experiments.

The reminder of the thesis is organized as follows. In chapter 2 a survey of relevant literature is reported. The model is then explained in detail in chapter 3 and in chapter 4 we present the instances generated. chapter 5 summarizes all the experiments performed and finally chapter 6 presents the conclusions on the work.

Chapter 2

Literature review

Electric vehicles (EVs) and their charging infrastructures have been widely studied in the Transportation Science and Logistics literature (Shen et al., 2019, Erdelić and Carić, 2019). Even if Vehicle-to-Grid (V2G) technologies have always been considered as a tool to increment the usage of EVs, they are not widely explored yet (Sovacool et al., 2018). Sortomme and El-Sharkawi, 2010 used vehicles with V2G technologies as a tool to control some aspects of the grid, called ancillary services, such as the load regulation and the spinning reserves. The optimization of the V2G assets is perform by an aggregator whose profit increases with regulation services. Zhang et al., 2021 embedded V2G technologies into an EV sharing. They formulated a two-stage stochastic IP model to optimize over the service opening, the capacity design and the fleet allocation under uncertainties. In the setting of a smart grid with heterogeneous charging facilities, Tang et al., 2017 proposed a model to jointly optimize the routing and charging scheduling. They adopted a distributed algorithm to ensure independence and privacy of the EV drivers. This problem has been extended by Triviño-Cabrera et al., 2019, to include also battery degradation. These authors introduced an agent in conjunction with the grid aimed at maximizing the drivers revenues.

With the progressive electrification of the public transports (PT), the interest in electric buses (EBs) is increasing as well (Deng et al., 2019). The electric conversion of fleets poses several questions regarding the fleet itself and the charging equipment. Several authors tackled this problem from a strategic planning perspective. At this aim, An, 2020 proposed a strategic plan taking into account the bus fleet size, time-of-use electricity price and stochastic charging demands. The same problem is tackled in S. Pelletier, Jabali, Mendoza, et al., 2019, where several scenarios for electric targets, EBs characteristics and type of chargers are considered. Other approaches instead, integrated a charging plan strategy to a vehicle routing problem for the buses. Zhou et al., 2020 developed a multi objective bi-level programming model for a mixed bus system fleet recharging at a single depot, optimizing both vehicle scheduling and charging scheduling and developed an efficient algorithm. The same problem, but with multiple depots and charging technologies is tackled by Yıldırım and Yıldız, 2021. Y. Wang et al., 2017 proposed a model for both a charging schedule procedure and a planning for the charging stations and charger purchase. Furthermore this model is applied in a real case study setting in Davis, California. Finally, Abdelwahed et al., 2020 proposed a MILP formulation to

optimize the opportunity fast-charging schedule of a fleet of EBs, minimizing the energy costs and the impact on the grid.

The Electric Vehicle Scheduling Problems (E-VSPs) is probably the most similar problem to the one of this work. In these problems the charging scheduling process is tackled while solving an assignment problem of routes. Wen et al., 2016 propose a MILP model to assign routes and minimize the total travel distances of EBs. In the model, the charge process of EBs is subordinated to the route assignment problem. EBs indeed are charged according to the time they stay in a station and the remaining battery charged. Furthermore, the recharging time is assumed to be a linear function of the amount of charged battery and no restrictions on the charger facilities are considered. In Yao et al., 2020 routes are assigned to a fleet of heterogeneous vehicles, and the authors solved an electric vehicle scheduling problem with multiple vehicle types (MVT-E-VSP) and optimizing both purchase and operational costs. For what concern the charging process itself however, the authors assumed that any type of EB is fully charged at the end of each route with a fixed cost and that each EB is provided with a fast charger. Alvo et al., 2021 adopted a two stage approach to solve the problem, minimizing the number of diesel buses employed in an heterogeneous fleet. They extended the previous setting by adding more flexibility in the charging process. Parallel charging of vehicles is limited by the number of chargers at the depot and the partial charging is allowed. However, the state of charge of vehicle is assumed to be linear in the charging time. In particular they considered a heterogeneous fleet of EBs and diesel buses and aim at minimizing the number of diesel buses employed. Janovec and Koháni, 2019 develop a linear model once again assigning routes to the smallest number of EBs. In particular they allow charging at multiple locations and introduced constraints on the number of chargers. The energy charged is linear in the charging time. It is also interest to notice that authors aimed at limiting the battery degradation effect by means of low values for the state of charge of vehicles. Nevertheless, an actual estimation of the degradation is ignored. Different charging strategies are analyzed in Spitzer et al., 2019. The authors deeply focused on analyzing the load of low voltage distribution grids and provided charging schedules feasible with respect to them. Among the scenarios presented, some of them aimed at minimizing charging costs of energy under time varying prices, others focused on the load of the grid. However, vehicles are still assumed to be fully charged before every route. A model which relies on the wireless charging of the on-line electric vehicle (OLEV) technology is developed by Jang et al., 2015. Still on the base of wireless charging, Yang et al., 2017 presented a model to minimize energy costs in the day ahead market. These two works however, are not really comparable with ours since they deeply depend on the wireless technologies which are not employed in this setting.

The problem analyzed in this work fits exactly in none of the field described. No strategic decisions regarding the fleet compositions are done indeed, as in the real scenario considered these decisions have already been made. Given the high complexity of VRPs, in order to make them feasible, usually many simplification are done regarding the charging process. On the other hand, the work presented here, deeply focuses on the charging process. The main characteristics of the work are inherited from Pelletier et al., 2018. Here, a charge scheduling process for a fleet of electric freight vehicles (EFV) is developed to optimize the operational

costs of the grid and the degradation of batteries. Simulations from the model battery of Tremblay et al., 2007, provide an approximation of a piece-wise linear charging process. As a results, the level of charge is non-linear with respect to the time. Furthermore, they include energy time variant prices and a fixed cost for the maximum power. In this work V2G technologies are incorporated in the fleet of EBs. Even if V2G technologies can be embedded directly in the model of Pelletier et al., 2018, in this work an enhanced version of this model is considered.

Table 2.1 summarises the features of the main works related with this thesis. In particular, it emphasizes how this work ignores the strategic planning of the fleet but focuses deeply on the charging process.

Reference	Strategic fleet composition	Routes assignment	Piece-wise linear charging	#chargers	Time-energy €	V2G
Wen et al., 2016	✗	✓	✗	✗	✗	✗
Yao et al., 2020	✓	✓	✗	✗	✗	✗
Alvo et al., 2021	✗	✓	✗	✓	✗	✗
Janovec and Koháni, 2019	✗	✓	✗	✓	✗	✗
Spitzer et al., 2019	✗	✗	✗	✓	✓	✓
Pelletier et al., 2018	✗	✗	✓	✗	✓	✗
EEV-CSP-V2G	✗	✗	✓	✓	✓	✓

Table 2.1: Summary of the related literature

Chapter 3

The EEV-CPS-V2G problem

In this chapter we introduce the enhanced electric vehicle charge scheduling problem with V2G technologies (EEV-CSP-V2G), starting from the electric vehicles charging scheduling problem (EV-CSP) of Pelletier et al., 2018. As already said, this problem aims at charging a fleet of EFV. Particular attention of the work is devoted to model the charging process itself. The state of charge (SOC) of EFVs is approximated as a piece wise linear function of time, depending on the current and the battery capacity. Hence, more accurate values for the SOC values are attained and at the same time overcharging is avoided. A quick review of the main battery models is presented in section 3.1. The charging process resulting from it is then presented in section 3.2. Another important aspect is the model of the degradation costs. The author exploited the approach followed by Han et al., 2014, which is explained in section section 3.3. We describe in details the problem setting in section 3.4. In section 3.5 we present the EV-CSP model and in section 3.6 its enhanced version. Finally in section 3.7 we introduce V2G technologies and we present the EEV-CPS-V2G model. The heuristic approach developed is then reported in section 3.8

3.1 Model battery review

The easiest model of a battery is a simple circuit with a voltage source V_{OC} in series with a resistance R (Figure 3.1). It follows that the battery instantaneous
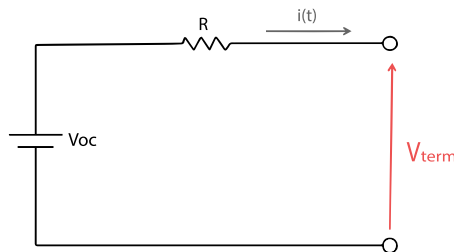
Figure 3.1: Simplest battery representation (adapted from Larminie and Lowry, 2012)

actual voltage is connected with the other terms with the relation

$$V_{term}(t) = V_{OC}(t) - Ri(t) \tag{3.1}$$

The model of the open voltage V_{OC} is therefore pivotal in the battery model itself. As reported in the detailed description of Larminie and Lowry, 2012, typically the open voltage depends on the number of cells and the depth of discharge DoD, where the former a parameter known from the manufacturer of the battery itself and the latter is modeled from the Peukert Capacity. The resistance is assumed to be dependent on the SOC and changes with the flow of the current. Instead of modeling the open voltage circuit, other approaches exploit pre-estabilished mathematical relationships, as in Shepherd, 1965. The author obtains the equation for the V_{OC} by monitoring the charging and discharging process of a battery. In his model battery the resistance R and the intensity of the current flowing are assumed to be constant during time, while specific behaviours on the polarization and the material of anode and cathode are assumed. The equation obtained is 3.2:

$$V_{OC} = V_c - K \left(\frac{Q}{Q - it} \right) i \qquad (3.2)$$

where V_c is a simplified form of a constant potential, K is the coefficient of polarization of the cathode, Q is the residual capacity on the cathode or anode. Equation 3.2 is then substituted into Equation 3.1, which is used to simulate curves. From the comparison of the simulated with the real ones, a new term can be added to take into account an initial drop of potential and correct the simulations. The resulting equation from Shepherd (1965) becomes

$$V_{OC} = V_c - K \left(\frac{Q}{Q - it} \right) i + A \exp\left(-Bit \right) \qquad (3.3)$$

where A and B are parameters that depend on the exponential zone that was missing in the first comparison of the curves mentioned before. Furthermore, the author provides the reader with a procedure to approximate the parameters from the discharging curves of the batteries. The main drawback of the equation proposed by Shepherd (1965) is that the non linear term in 3.3 causes an algebraic loop in simulation phase making this model unmanageable. On the other hand, these equations are very interesting since they model both charge and discharge processes. The work of Tremblay et al., 2007 extends Shepard's equations by modifying the non linear term in 3.3. The equation deriving from it is the following:

$$V_{OC}(t) = V_c - K \left(\frac{Q}{Q - \int idt} \right) + A \exp\left(-B \int idt \right) \qquad (3.4)$$

which can be further modified. Letting $\frac{1}{SOC(t)} = \frac{Q}{Q - \int idt}$, it follows $\int idt = Q(1 - SOC(t))$ and by substitution we get

$$V_{OC}(t) = V_c - \frac{K}{SOC(t)} + A \exp\left(-BQ(1 - SOC(t)) \right) \qquad (3.5)$$

It is interesting to notice the definition of the SOC:

$$SOC(t) = \frac{Q - \int idt}{Q} \qquad (3.6)$$

as it is indeed the amount of charge the battery contains divided by its maximum charge capacity Q. Finally we obtain the equation of terminal voltage both for charging and discharging reported in Pelletier et al., 2018

$$V_{term}(t) = V_c - \frac{K}{SOC(t)} + A\exp\left(-BQ\left(1 - SOC(t)\right)\right) - Ri(t) \qquad (3.7)$$

then letting $OVC = V_{OC}$, the equation of Pelletier et al. (2018) is obtained:

$$V_{term}(t) = OVC(SOC(t)) - Ri(t) \qquad (3.8)$$

It is important to remark that the equation derived in Shepherd, 1965 holds both for charging and discharging, as well for the extension of Tremblay et al., 2007. It follows that all the charging processes that exploit such a battery model, are valid in both the directions.

3.2 Charging process

To prevent batteries from degradation, they are typically charged under a CC-CV regime which is made up of two phases. In the first one the charging current that flows in the battery is kept constant (CC). Because of the battery model assumed, the current, terminal voltage and SOC are linked according to Equation 3.8. In particular if i(t) is constant in the definition of SOC (3.6), the integral becomes just the product it leading to $SOC(t) = 1 - \frac{i}{Q}t$. Namely the SOC is linear in the time when the current is constant and it has coefficients $\frac{i}{Q}$. Hence, during the CC phase, by setting $i(t) = i_{CC}$ in Equation 3.8 and in Equation 3.6, the $SOC(t)$ itself is linear in t with a coefficient of i_{CC}/Q, while the terminal voltage increases according to the $OVC(SOC(t))$. To avoid damages to the battery, the terminal voltage cannot be greater than V_{CV}. Once reached, this value is kept constant and the constant voltage (CV) phase starts. Here the current decreases with time while the $SOC(t)$ is no more linear but still increases. As already remarked, the CC-CV curve can be used both the directions. As in Pelletier et al., 2018, a piece-wise approximation of the curve is employed to model $SOC(t)$. In this way, in every segment, the SOC is linear in t with respect to a coefficient given by the maximum current applied in that piece divided by Q.

3.3 Degradation costs

The investment in batteries and their replacements have an high impact on the overall costs of the fleet. Modeling the impact on the total operational costs could therefore lead to a better charging schedule. In this section the approach used to model them is described.

Lithium-ion batteries are subjected to two types of degradation which both affect their actual life duration. Battery life can be estimated with the *calendar life*, which is mainly related with its storage, or with the *cycle life*, that counts the number of charge-discharge cycles available before its capacity goes below the 80%. Since
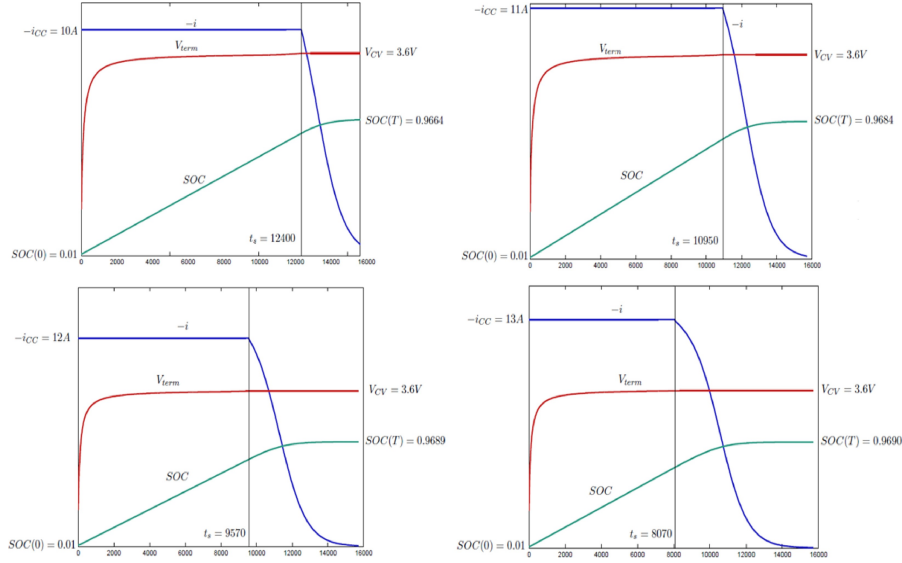
Figure 3.2: Examples of CC-CV curves (source: S. Pelletier, Jabali, Laporte, et al., 2017)

calendar life is independent on the charging schedule followed (Farzin et al. (2016)), in this work only the second contribution is modeled.

Cycle life is mainly related with the loss of active lithium ions. While developing their model for charge/discharge, Ning et al. (2006) explained that the loss of active lithium ions is due to electrochemical solvent reduction reaction at anode/electrolyte interface. With a physic approach it is possible to model these electrochemical reactions as a function of the operational conditions. The performance of batteries is then simulated by means of analytical methods. Aside from this approach, in literature there are models for the cycle life estimation neglecting the internal chemical interactions occurring in the charge/discharge process. This second type of approach is followed here, in particular the one adopted in Han et al., 2014 which is now described.

In order to develop a battery model degradation, several experiments on batteries are necessary. The high costs of experiments result in poor data for batteries. However, among them, the curve of the number of achievable cycle count (ACC) with respect to the depth-of-discharge (DOD) is always available. ACC-DOD curves (Figure 3.3) are the only manufacturing data exploited in Han et al., 2014.

From these curves, the authors develop a *wear density function* (WDF) which express a cost for the usage of battering while charging/discharging and uses as control parameter the state of charge of the vehicle (SOC) and its variation. For an accurate model of the battery wear, several parameters should be incorporated. Firstly, the SOC needs to be accounted for as it is strictly related with the battery wear and is also linked to the DOD. In principle, also the temperature should be considered as its variation may have an impact on the battery wear. However, for most applications, temperature itself can be easily omitted. It is enough to use experimental data obtained under the working temperature of the application. As result, the wear cost function depends only on the transferred energy (ΔkW) and
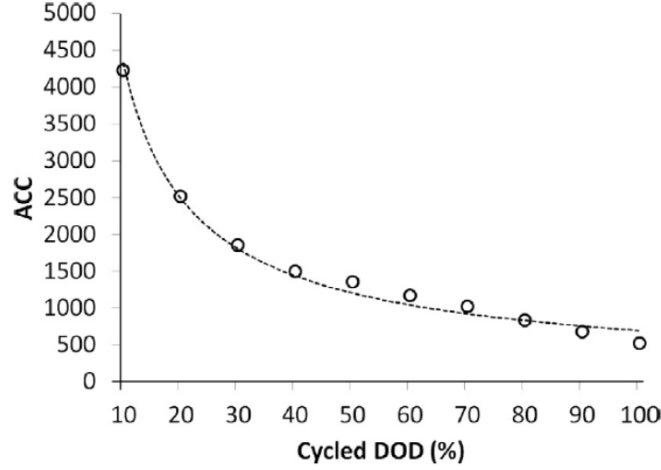
Figure 3.3: Example of a manufacturing ACC-DOD curve for a lithium-ion battery (source: Han et al., 2014)

the SOC:

$$WearCost = W(\Delta kW, SOC) \tag{3.9}$$

Starting from the ACC-DOD curve, the authors first derive an average wear cost (AWC) per unit of energy transferred [$/kWh]. In particular, this cost is the ratio between the initial battery price and the total energy transferable during the life cycle. This last term can be computed as the quantity of energy transferable during every cycle times the number of cycles. Then it is corrected with a factor μ which represents the efficiency of the process. The energy transferred in a cycle depends on the depth of discharge that we reach and it is $D \cdot BatterySize$. The number of cycle instead is obtainable from the ACC-DOD curve. As discharging needs to be considered too, this number is doubled.

$$AWC(D) = \frac{BatteryPrice}{2 \cdot ACC(D) \cdot D \cdot BattterySize \cdot \mu^2} \tag{3.10}$$

AWC costs do not take into account the interval of SOC in which the charge/discharge process happens and assumes that the battery is always full when discharge happens. Since in most applications various ranges of SOC are employed, the authors extend this method. They introduce a wear density function (WDF) in order to express the AWC cost as the integral mean of this function. Therefore it holds the relation:

$$AWC(D) = \frac{1}{D} \int_{1-D}^{D} W(s)ds \tag{3.11}$$

By substituting this equation in Equation 3.10, it is possible to fit the function W(s). Once obtained the wear cost density function, degradation costs are computed by means of the following expression:

$$TotalWearCost = BatterySize \cdot \int_{0}^{T} W\left(SOC(t)\right) |\frac{dSOC(t)}{dt}|dt \tag{3.12}$$

To get a discrete version of the wear cost function, the procedure is really similar and it starts again from Equation 3.10. The average wear cost function then is modified to take into account the different states of charge of EVs, namely Equation 3.11 becomes

$$AWC_e(D) = \frac{1}{D} \sum_{s=1-D}^{1-\Delta s} W_d(s) \Delta q(s) \tag{3.13}$$

where Δq is the energy corresponding to Δs and $W_d(s)$ is the cost of transferring the energy in the SOC from range s to $s + \Delta s$. When substituting it in Equation 3.10, the $BatterySize$ at the denominator simplifies with the one in Equation 3.13. Equation 3.10 becomes then:

$$\frac{1}{D} \sum_{s=1-D}^{1-\Delta s} W_d(s) \Delta q(s) = \frac{BatteryPrice}{2 \cdot ACC(D) \cdot D \cdot \mu^2} \tag{3.14}$$

and isolating W_d

$$\sum_{s=1-D}^{1-\Delta s} W_d(s) = \frac{BatteryPrice}{2 \cdot ACC(D) \cdot \sum_{s=1-D}^{1-\Delta s} \Delta q(s) \cdot \mu^2} \tag{3.15}$$

Once fixed a number of breakpoints $\mathcal{D}$ each one of length Δs, from Equation 3.15 is possible to obtain the system

$$\begin{bmatrix} 1 & 0 & 0 & \dots & 0 \\ 1 & 1 & 0 & \dots & 0 \\ \vdots & \vdots & \vdots & \vdots & \vdots \\ 1 & 1 & 0 & \dots & 0 \end{bmatrix} \begin{bmatrix} W_d(1 - \Delta s) \\ W_d(1 - 2\Delta s) \\ \vdots \\ W_d(0) \end{bmatrix} = \begin{bmatrix} \frac{BatteryPrice}{2 \cdot ACC(D) \cdot \Delta q(1 - \Delta s) \cdot \mu^2} \\ \frac{BatteryPrice}{2 \cdot ACC(D) \cdot \sum_{s=1-D}^{1-2\Delta s} \Delta q(s) \cdot \mu^2} \\ \vdots \\ \frac{BatteryPrice}{2 \cdot ACC(D) \cdot \sum_{s=0}^{1} \Delta q(s) \cdot \mu^2} \end{bmatrix}$$

which solution is the discretized wear cost function.
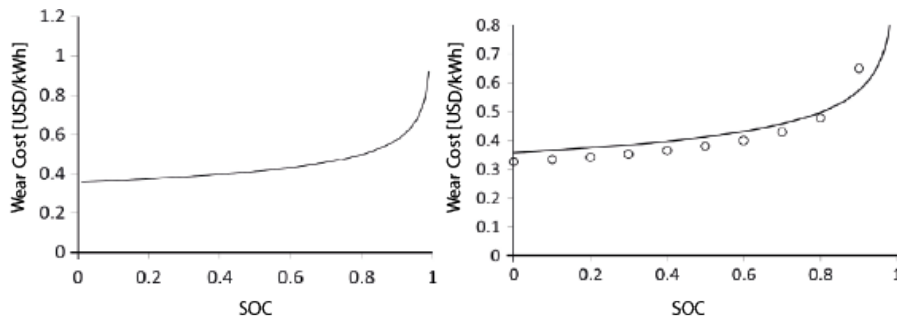
Figure 3.4: From Han et al., 2014: example of a continuous and discrete wear cost function for a a 16-kW h, $10,000 battery obtained from ACC-DOD curve in Figure 3.3
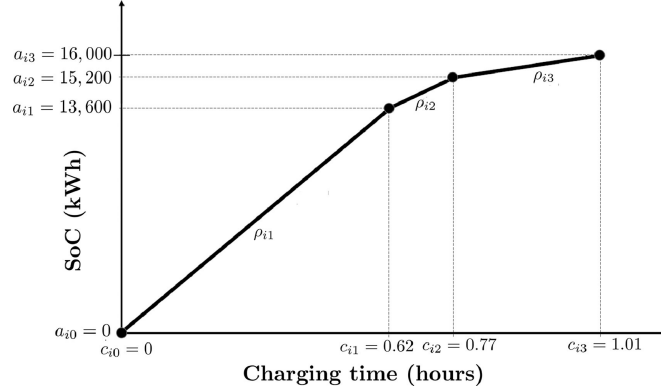
Figure 3.5: CC-CV curve (source: Froger et al., 2019)

3.4   The EEV-CPS-V2G setting

The charging plan is over a day divided in a set of discrete periods $\{1 \ldots n_p\}$, each one of δ duration. A homogeneous fleet of EV is given and it is formalized in the set $\mathcal{K}$. Each EVs is provided with a battery of charge capacity Q and E energy capacity. The routes to be performed in the planning horizon are known in advanced and indexed on $\mathcal{R}$. So we know the first route they have to perform f_k as well as the last one l_k. For each route, the departure β_r period, the arrival α_r one as well as their SOC consumption ΔSOC_r are known. Furthermore they are assigned to a vehicle of the fleet.

Vehicles can be charged with the chargers available in the depot. There are s different types of chargers represented in the set $\mathcal{S}$. For each type, a given number of chargers κ_s is available. The charging process is modeled as a piece-wise linear approximation of the CC-CV curve similar to Froger et al., 2019 (Figure 3.5). For each charger type s, a set of breakpoints $\mathcal{B}_s$ is given. The SOC is then divided into b_s intervals, leading to $b_s + 1$ different values of SOC a_{si} is associated. In every interval of the curve the SOC is linear in the time with slope given by a value of the current I_{si} over the battery capacity Q. Furthermore, the usage of a charger requires a power P_s from the grid.

In a real application, it can happen that EVs must be positioned in dedicated spaces of the depot in order to be charged. It is therefore preferable to avoid a frequent swap of chargers and EVs. For this reason, we assume that the EVs can be plugged in at most C times before every route. When a vehicles starts charging, we will refer to it as a "charging event".

The energy plan adopted includes two different types of costs: a cost per period c_p and a cost F depending on the maximum power retrieved in the planning period. The grid can support a maximum charge G. Along with these costs, there are the ones related to the battery degradation phenomena. They are calibrated into D points of the SOC and are expressed as w_d. The length of each interval is L.

In this problem there are several types of costs to be taken into account. The first one is a cost per period c_p. This cost depends on the quantity of energy requested from the grid in every period to charge the vehicle. Namely, it is related with the energy that enters the vehicles: if a vehicle charges q KWh at period p, this will costs $c_p \cdot q$, then all the EVs and all the periods must be considered. The

second one instead is related with the maximum power retrieved from the grid. In every period, it is necessary to consider the power requested to the grid: the maximum value among all periods is then multiplied by the facility related demand (FDR) cost F. Finally, in order to calibrate the wear cost function in Equation 3.15 the set of points $\mathcal{D}$, every point of this set is associated with an interval of SOC upper bounded by δ_d. Since everything we charge in the vehicle also needs to be discharged, the costs $w(s)$ need to be doubled. To compute the total degradation costs, it is necessary to multiply every point in the discrete function with the quantity of energy used in that range during the whole planning. These three costs need to be modeled and the total costs is given by their sum. A complete list of the used parameters is found in Table A.1 of the appendix.

To solve this problem is necessary to schedule the charge of EVs. This means deciding for every period in the planning horizon whether to charge or not a vehicle. Furthermore, if an EV is charged, we must choose the type of charger to use and how much to charge. Of course the charging process will aim at minimizing the three types of costs described, but at the same time there are important conditions to be taken into account. For sure vehicles cannot be charged when they are not in the depot and their charge must guarantee that they are able to perform the routes assigned every time they leave the depot. At the same time the level of charge must be in a proper range. While charging, every vehicle must be connected with one and only one charger considering the availability of each type in the depot. To guarantee a realistic planning, it is better to avoid plugging and unplugging an EV frequently. Then, for what concerns degradation costs, it is necessary to compute the SOC actually charged in every interval used to calibrate the wear cost function.

Lastly, it is necessary to monitor the charging process following the CC-CV curve. In section 3.5 we present the EV-CSP model of Pelletier et al., 2018. In section 3.6, we propose a number of enhancements of the EV-CSP model. In section 3.7 we integrate V2G technologies in the EEV-CSP model, resulting in the EEV-CPS-V2G model.

3.5 EV-CSP

In this model, EVs are assumed to be charged with a slope that can be smaller than the one in the CC-CV approximation. Thus, we may have a different value of the current for every piece of the curve. The current which enters in an EB cannot be larger that the corresponding value. With this aim, the set of real positive variables i_{pk} is used to measure the current entering the vehicle k in period p, together with the set of binary variables x_{pksi} that is used to control whether vehicle k is charging at time p along the ith segment of the CC-CV curve of charger type s. This happens when the SOC of k is between $a_{s,i-1}$ and $a_{s,i}$. The SOC of EVs is monitored at every period p for each vehicle k by means of variables SOC_{pk}. The real positive variable y measures the peak of energy and is used to compute the FRD costs. Charging events are counted with the binary variables z_{pk} that have value 1 if the vehicle k starts being charged during period p. The variables soc^+_{rd} and u^+_{rd} are used to split the SOC charged before every routes into the proper interval of $\mathcal{D}$. For a complete list of variables we refer the reader to Table A.2 of

the Appendix A.

We present now the MILP formulation of the EV-CSP model.

$$\min \sum_{p \in P} \sum_{k \in K} c_p \cdot E \cdot \frac{\delta i_{pk}}{Q} + F \cdot y + \sum_{r \in R} \sum_{d \in D} 2w_d E \cdot soc_{dr}^+ \tag{3.16}$$

$$\text{s.t.} \quad \sum_{p=\beta_r}^{\alpha_r} \sum_{s \in S} \sum_{i \in B_S \setminus \{0\}} x_{pv_r si} = 0 \qquad r \in R \tag{3.17}$$

$$\sum_{k \in K} \sum_{i \in B_s \setminus \{0\}} x_{pksi} \leq \kappa_s \qquad p \in P, s \in S \setminus \{0\} \tag{3.18}$$

$$\sum_{s \in S} \sum_{i \in B_s \setminus \{0\}} x_{pksi} \leq 1 \qquad k \in K, p \in P \tag{3.19}$$

$$0 \leq i_{pk} \leq \sum_{s \in S} \sum_{i \in B_s \setminus \{0\}} I_{si} \cdot x_{pksi} \qquad k \in K, p \in p \tag{3.20}$$

$$SOC_{p+1,k} \leq a_{s,i} + 1 - x_{pksi} \qquad k \in K, p \in P, s \in S, i \in B_s \setminus \{0\} \tag{3.21}$$

$$SOC_{p,k} \geq a_{s,i-1} - 1 + x_{pksi} \qquad k \in K, p \in P, s \in S, i \in B_s \setminus \{0\} \tag{3.22}$$

$$SOC_{p,k} = SOC_{p-1,k} + \frac{i_{p-1,k}}{Q} \cdot \delta \qquad k \in K, p \in P \setminus \{0\} \tag{3.23}$$

$$SOC_{\alpha_r,v_r} = SOC_{\beta_r,v_r} - \Delta SOC_r \qquad r \in R \tag{3.24}$$

$$SOC_{0k} = S\hat{O}C_{0k} \qquad k \in K \tag{3.25}$$

$$SOC_{min} \leq SOC_{pk} \leq SOC_{max} \qquad k \in K, p \in P \tag{3.26}$$

$$\sum_{k \in K} \sum_{s \in S} \sum_{i \in B_s \setminus \{0\}} P_s \cdot x_{pksi} \leq y \qquad p \in P \tag{3.27}$$

$$0 \leq y \leq G \tag{3.28}$$

$$z_{pk} \geq \sum_{i \in B_s \setminus \{0\}} x_{pksi} - \sum_{i \in B_s \setminus \{0\}} x_{p-1,ksi} \qquad k \in K, p \in P \setminus \{1\}, s \in S \tag{3.29}$$

$$z_{1k} \geq \sum_{i \in B_s \setminus \{0\}} x_{1ksi} \qquad k \in K, s \in S \tag{3.30}$$

$$\sum_{p=\alpha_{\eta_r}}^{\beta_r - 1} z_{pv_r} \leq C \qquad r \in R \tag{3.31}$$

$$\sum_{d \in D} soc_{dr}^+ = SOC_{\beta_r v_r} - SOC_{\alpha_{\eta_r},v_r} \qquad r \in R \tag{3.32}$$

$$soc_{dr}^+ \leq \bar{\delta}_d - SOC_{\alpha_{\eta_r},v_r} + \left(1 - u_{dr}^+\right)\left(1 - \bar{\delta}_d\right) \qquad d \in D, r \in R \tag{3.33}$$

$$0 \leq soc_{dr}^+ \leq L \cdot u_{dr}^+ \qquad d \in D, r \in R \tag{3.34}$$

$$0 \leq SOC_{pk} \leq 1 \qquad k \in K, p \in P \tag{3.35}$$

$$y \geq 0 \tag{3.36}$$

$$x_{pksi} \in \{0,1\} \qquad k \in K, p \in P, s \in S, i \in B_s \setminus \{0\} \tag{3.37}$$

$$z_{pk} \in \{0,1\} \qquad k \in K, p \in P \tag{3.38}$$

$$0 \leq soc_{dr}^+ \leq 1 \qquad d \in \mathcal{D}, r \in \mathcal{R} \tag{3.39}$$

$$u_{dr}^+ \in \{0,1\} \qquad d \in D, r \in R \tag{3.40}$$

The objective function (3.16) minimizes the total costs given by the energy costs, FRD costs and degradation costs. Constraints (3.17) forbid charging EVs while they are outside the depot. The connection of EVs to the grid needs to take into account the number of each type of charger (3.18) and each vehicle must be connected only to one charger (3.19). The block of constraints (3.20) - (3.24) is used to model the charging process. First of all, the charging current that flows in an EV during a period is bounded by the current of the corresponding segment of the CC-CV curve (3.20); then the values of SOC during the charging must lie inside the proper interval of SOC ((3.21)-(3.22)). Finally, if an EV is charged, its SOC is increased according to constraint (3.23). The SOC consumption due to the routes is accounted in (3.24). Furthermore, we assume that the initial value of the SOC is given (3.25) and we ensure that the SOC is inside a range for the whole period (3.26). Constraints (3.27) set the maximum power, while (3.28) ensures that grid capacity is not exceeded. Constraints (3.29) - (3.30) are employed to count the charging events whose number is bounded in (3.31). Constraint (3.32) ensures that while considering degradation costs, all the SOC charged before the route is taken into account. Then (3.33) and (3.34) split the variation into the proper interval of $\mathcal{D}$, exploiting the monotonicity of the wear cost function. Finally in (3.35) - (3.40) all the variables domains are specified.

3.6 EEV-CSP

Starting from the model of Pelletier et al., 2018, we developed an enhanced electric vehicle charge scheduling problem (EEV-CSP). In particular, in our formulation we propose a more accurate approach to model the charging process and a more realistic charging routine for the schedule itself.

3.6.1 Charging process in the EEV-CSP

Our first contribution is in the charging process approximation. As already mentioned, the charging process follows a CC-CV curve and the SOC is a piece-wise linear function of time. However, the set of variables used in Pelletier et al., 2018 model, have the effect of limiting the charging process in reality. Assume for instance that during period p vehicle k is charging. We assume that it uses charger s and that the SOC of the vehicle is within the interval $[a_{s,i-1}, a_{si}]$, meaning that the binary variable x_{pksi} is equal to 1. Assume also that the value of SOC is really close to the upper bound a_{si}. What happens in practice is that the model will force the value of the current in that period i_{pk} to be such that the SOC at the end of the period will be exactly equal to a_{si}. Then, in the next period, the SOC will belong to the next interval, variable $x_{pks,i+1}$ will be 1 and, if it is what the schedule was prescribing, the charging process will go on according to the next segment of the CC-CV curve.

In practice, in Pelletier et al., 2018, by allowing to charge only along one segment of the CC-CV curve in a single period, some periods at the depot are wasted as they are just used to reach the proper breakpoint. With our EEV-CSP model, we aim at relaxing this assumption allowing the usage of two or more consecutive

segments during a given period. In order to do this, we assume that the charging current that we use to charge to the EBs is always equal to the one in the CC-CV approximation. Therefore, the set of variables i_{pk} of EV-CSP are not employed. On the other hand, in order to model this more realistic charging process, we need to introduce new variables. We use the set of real variables Φ_{pksi} to control the quantity of SOC that is charged in vehicle k at time p the s charger along segment i. Then we introduce the set of binary variables q_{pks} defined like 1 if vehicle k uses the charger type s during period p, 0 otherwise.

Notice that, since we are no longer using the variables for the current, we need to compute the energy withdrawn from the grid with these new variables. As variables Φ_{pksi} express the increase of SOC of vehicles, in order to know the energy used during a time period p, it is enough to multiply by the battery capacity E with the total increase of SOC during that period p. The energy contribution (3.41) for the objective function becomes then

$$\sum_{p \in P} \sum_{k \in K} c_p E \sum_{s \in \mathcal{S}} \sum_{i \in B_s \setminus \{0\}} \Phi_{pksi}. \tag{3.41}$$

Then, we model the new charging process. First of all, we omit the assumption that the charging happens along one segment only, namely constraints (3.19) and we impose that only one type of charger can be used in every period by a vehicle, as it is written in Equation 3.42

$$\sum_{s \in S} q_{pks} \leq 1 \qquad p \in \mathcal{P}, k \in \mathcal{K} \tag{3.42}$$

Then for sure the usage of a charger along its segments needs to be linked with the usage of the charger itself. These coherence constraints are modeled in (3.43) and (3.44).

$$q_{pks} \geq x_{pksi} \qquad p \in \mathcal{P}, k \in \mathcal{K}, s \in \mathcal{S}, i \in B_s \setminus \{0\} \tag{3.43}$$

$$q_{pks} \leq \sum_{i \in B_s \setminus \{0\}} x_{pksi} \qquad p \in \mathcal{P}, k \in \mathcal{K}, s \in \mathcal{S} \tag{3.44}$$

In particular, we are imposing that whenever we use a segment we must consider the associated charger as used (Equation 3.43). Also if we use a charger at time p, then the charging process needs to be on at least one of its segments (Equation 3.44). The constraints of EV-CSP that ensure that the SOC is in the correct interval ((3.21)-((3.22)) then must be modified. Indeed we need to make sure that every time that the segment i is changed we have reached the upper bound a_{si}. At the same time we need to be sure that we are not charging more than what we can along one segments. These conditions are expressed in the new constraints (3.45) and (3.46).

$$SOC_{pk} + \sum_{i' \leq i} \Phi_{pksi'} \leq a_{si} x_{pksi} + (1 - x_{pksi}) \qquad p \in \mathcal{P}, k \in \mathcal{K}, s \in \mathcal{S}, i \in B_s \setminus \{0\} \tag{3.45}$$

$$SOC_{pk} + \sum_{i' < i} \Phi_{pksi'} \geq a_{s,i-1} x_{pksi} + (x_{pksi} - 1) \qquad p \in \mathcal{P}, k \in \mathcal{K}, s \in \mathcal{S}, i \in B_s \setminus \{0\} \tag{3.46}$$

We also add (3.47) to link the variables that express the usage of a segment and obtain a bound on the SOC that can be charged along each segment.

$$\Phi_{pksi} \leq (a_{si} - a_{s,i-1})x_{pksi} \qquad p \in \mathcal{P}, k \in \mathcal{K}, s \in \mathcal{S}, i \in B_s \setminus \{0\} \qquad (3.47)$$

In order to have a correct model then, we need to be sure that the SOC the we charge in the vehicles during a period is actually obtainable from the grid. Indeed, we have assumed that the level of current applied is fixed and we have only modeled the SOC that is charged in the vehicles. However, as it is clear from the charging process approximation, given the level of current I_s, a certain time is needed to obtain the desired increase of SOC. We need to ensure that the required time in every period, is not longer than the length of the period itself δ. This can be expressed by adding Equation 3.48

$$\sum_{s \in \mathcal{S}} \sum_{i \in B_s \setminus \{0\}} \frac{\Phi_{pksi}}{I_{si}} Q \leq \delta \qquad \forall p \in \mathcal{P}, k \in \mathcal{K}, \qquad (3.48)$$

which indeed ensures that the charging process lasts less than the period itself. Finally, the SOC at the end of period p becomes simply the sum of the SOC at the beginning of period p and the SOC charged during p (Equation 3.49).

$$SOC_{p+1,k} = SOC_{pk} + \sum_{s \in \mathcal{S}} \sum_{i \in B_s \setminus \{0\}} \Phi_{pksi} \qquad \forall p \in \mathcal{P} \setminus \{n_p\}, k \in \mathcal{K}, \qquad (3.49)$$

3.6.2 Cyclic charging schedule

In the EV-CSP model the original time horizon is of 3 days. Even if it is still short, this length allowed the authors to make a strong distinction between the initial time of the planning horizon and the final one. For instance, they assume that the initial SOC is known for all the EVs. No assumptions are made instead on the final SOC.

Recall then, that when it is in the depot there is a limitation in the number of times that an EV can be plugged in. In the model of Pelletier et al., 2018, the number of charging event is bounded only before the routes.

In our EEV-CSP model instead, we consider the whole charging planning in a cyclic fashion. First of all, we assume that the initial SOC is equal to the final. Furthermore, we do not set an initial level of SOC for the EVs but we let the model decide it. Then, we do not split the count of charging event based on the end of the time horizon, but we just base it on the departures from the depot. To clarify this concept, let us make an example. Suppose that the EV k has to perform only one route that starts at period 4 and ends at 20. We will impose that the number of charging events from period 20 to the end of the time horizon and from the beginning of the time horizon up to period 4 is strictly less than C, where C is the maximum number of charging events.

With this idea, as we have already imposed that what happens during period p influences what happens at period $p + 1$, we do the same for the final period in the horizon n_p and the initial period 1. Therefore, we modify the formulation to account for as follows ((3.50)-(3.53)).

$$SOC_{1k} = SOC_{n_p k} + \sum_{s \in \mathcal{S}} \sum_{i \in B_s \setminus \{0\}} \Phi^+_{n_p ksi} \qquad k \in \mathcal{K} \tag{3.50}$$

$$z_{1k} \geq q^+_{1ks} - q^+_{n_p ks} \qquad k \in \mathcal{K}, s \in \mathcal{S} \tag{3.51}$$

$$\sum_{p=\alpha_{\eta_r}}^{\beta_r - 1} z_{pv_r} \leq C \qquad r \in \mathcal{R} \setminus \{f_k | k \in \mathcal{K}\} \tag{3.52}$$

$$\sum_{p=\alpha_{l_k}}^{\beta_{f_k} - 1} z_{pk} \leq C \qquad k \in \mathcal{K} \tag{3.53}$$

In particular, in Equation 3.50 we link the initial SOC with the final SOC. Then, in Equation 3.51 we count the charging events at the initial period on the base of what happens in the final one. Equation 3.52 is similar to the one in the model of Pelletier et al., 2018 (3.31) as they both count the number of charging events before every route, but we exclude the earliest route for every EB. Indeed, the number of charging events before the first routes must be considered with the ones of the latest (3.73).

We report now the complete MILP formulation for the EEV-CSP . We remind the reader that the complete list of variables is in Appendix A.

$$\min \sum_{p \in P} \sum_{k \in K} c_p E \sum_{s \in \mathcal{S}} \sum_{i \in B_s \setminus \{0\}} \Phi_{pksi} + F \cdot y + \sum_{r \in R} \sum_{d \in D} 2w_d E \cdot soc^+_{dr} \tag{3.54}$$

$$\text{s.t.} \quad \sum_{p=\beta_r}^{\alpha_r} \sum_{s \in \mathcal{S}} q_{pv_r s} = 0 \qquad r \in \mathcal{R} \tag{3.55}$$

$$\sum_{k \in K} q_{pks} \leq \kappa_s \qquad p \in \mathcal{P}, s \in \mathcal{S} \tag{3.56}$$

$$\sum_{s \in S} q_{pks} \leq 1 \qquad p \in \mathcal{P}, k \in \mathcal{K} \tag{3.57}$$

$$q_{pks} \leq \sum_{i \in B_s \setminus \{0\}} x_{pksi} \qquad p \in \mathcal{P}, k \in \mathcal{K}, s \in \mathcal{S} \tag{3.58}$$

$$q_{pks} \geq x_{pksi} \qquad p \in \mathcal{P}, k \in \mathcal{K}, s \in \mathcal{S}, i \in B_s \setminus \{0\} \tag{3.59}$$

$$SOC_{\alpha_r, k_r} = SOC_{\beta_r, k_r} - \Delta SOC_r \qquad r \in R \tag{3.60}$$

$$SOC_{pk} + \sum_{i' \leq i} \Phi_{pksi'} \leq a_{si} x_{pksi} + (1 - x_{pksi}) \qquad p \in \mathcal{P}, k \in \mathcal{K}, s \in \mathcal{S}, i \in B_s \setminus \{0\} \tag{3.61}$$

$$SOC_{pk} + \sum_{i' < i} \Phi_{pksi'} \geq a_{s,i-1} x_{pksi} + (x_{pksi} - 1) \qquad p \in \mathcal{P}, k \in \mathcal{K}, s \in \mathcal{S}, i \in B_s \setminus \{0\} \tag{3.62}$$

$$\Phi_{pksi} \leq (a_{si} - a_{s,i-1}) x_{pksi} \qquad p \in \mathcal{P}, k \in \mathcal{K}, s \in \mathcal{S}, i \in B_s \setminus \{0\} \tag{3.63}$$

$$\sum_{s \in \mathcal{S}} \sum_{i \in B_s \setminus \{0\}} \frac{\Phi_{pksi}}{I_{si}} Q \leq \delta \qquad \forall p \in \mathcal{P}, k \in \mathcal{K} \tag{3.64}$$

$$SOC_{p+1,k} = SOC_{pk} + \sum_{s \in \mathcal{S}} \sum_{i \in B_s \setminus \{0\}} \Phi_{pksi} \qquad \forall p \in \mathcal{P} \setminus \{n_p\}, k \in \mathcal{K} \tag{3.65}$$

$$SOC_{1k} = SOC_{n_p k} + \sum_{s \in \mathcal{S}} \sum_{i \in B_s \setminus \{0\}} \Phi^+_{n_p ksi} \qquad k \in \mathcal{K} \tag{3.66}$$

$$SOC_{min} \leq SOC_{pk} \leq SOC_{max} \qquad p \in \mathcal{P}, k \in \mathcal{K} \tag{3.67}$$

$$\sum_{k \in \mathcal{K}} \sum_{s \in \mathcal{S}} P_s \cdot q_{pks} \leq y \qquad p \in \mathcal{P} \tag{3.68}$$

$$0 \leq y \leq G \tag{3.69}$$

$$z_{pk} \geq q_{pks} - q_{p-1,ks} \qquad p \in \mathcal{P} \setminus 0, k \in \mathcal{K}, s \in \mathcal{S} \tag{3.70}$$

$$z_{1k} \geq q^+_{1ks} - q^+_{n_p ks} \qquad k \in \mathcal{K}, s \in \mathcal{S} \tag{3.71}$$

$$\sum_{p=\alpha_{\eta_r}}^{\beta_r - 1} z_{pv_r} \leq C \qquad r \in \mathcal{R} \setminus \{f_k | k \in \mathcal{K}\} \tag{3.72}$$

$$\sum_{p=\alpha_{l_k}}^{\beta_{f_k} - 1} z_{pk} \leq C \qquad k \in \mathcal{K} \tag{3.73}$$

$$\sum_{d \in D} soc^+_{dr} = SOC_{\beta_r v_r} - SOC_{\alpha_{\eta_r}, v_r} \qquad r \in R \tag{3.74}$$

$$soc^+_{dr} \leq \bar{\delta}_d - SOC_{\alpha_{\eta_r}, v_r} + \left(1 - u^+_{dr}\right)\left(1 - \bar{\delta}_d\right) \qquad d \in D, r \in R \tag{3.75}$$

$$0 \leq soc^+_{dr} \leq L \cdot u^+_{dr} \qquad d \in D, r \in R \tag{3.76}$$

$$SOC_{min} \leq SOC_{pk} \leq SOC_{max} \qquad p \in \mathcal{P}, k \in \mathcal{K} \tag{3.77}$$

$$x_{pksi} \in \{0, 1\} \qquad p \in \mathcal{P}, k \in \mathcal{K}, s \in \mathcal{S}, i \in B_s \setminus \{0\} \tag{3.78}$$

$$\Phi_{pksi} \geq 0 \qquad p \in \mathcal{P}, k \in \mathcal{K}, s \in \mathcal{S}, i \in B_s \setminus \{0\} \tag{3.79}$$

$$y \geq 0 \tag{3.80}$$

$$z_{pk} \in \{0, 1\} \qquad p \in \mathcal{P}, k \in \mathcal{K} \tag{3.81}$$

$$0 \leq soc^+_{dr} \leq 1 \qquad d \in \mathcal{D}, r \in \mathcal{R}, \tag{3.82}$$

$$u^+_{dr} \in \{0, 1\} \qquad d \in \mathcal{D}, r \in \mathcal{R} \tag{3.83}$$

$$\tag{3.84}$$

3.7 EEV-CSP-V2G

From the literature review on the battery models in section 3.1, it follows that the battery model in EV-CSP and EEV-CSP can still be employed for bidirectional flow. In particular, the CC-CV process still holds. However, introducing V2G technologies to this setting, requires some changes. First of all, we assume that some EVs as well as some chargers support the bidirectional flow of current. Then, it is also necessary to understand how V2G technologies can affect the problem. Under this scenario, we assume that the set $\mathcal{H} \subset \mathcal{K}$ is a subset of EVs. We refer to the EV in $\mathcal{H}$ as EV-V2Gs. Furthermore, let $\mathcal{T} \subset \mathcal{S}$ be the set of chargers that support the bidirectional flow. The parameter η_{inv} is used for the dissipation of power from EV provided with V2G technologies (EV-V2Gs) towards the grid.

We consider also the energy that is needed for the operation of the depot is

given. Thus, we also assume now that the depot itself requires a certain amount of energy at every period π_p. The energy and the power related to the depot contribute as well to the total costs. The complete list of parameters is in Table A.1 in the Appendix.

The decisions to be taken in this scenario, are the same as the ones described in section 3.4. In addition, for each EV-V2Gs we have to decide whether it discharges some energy and how much.

Almost all the variables used in EEV-CSP are used, many of them are doubles to model the opposite flow of the current. The set of binary variables x^+_{pksi} is still used to model the charging process along the CC-CV curve when the current is entering the EV and x^+_{pksi} is the analogous for discharging. The SOC variation on every piece of the curve i for every charger s and every time p and vehicle k is monitored by Φ^+_{pksi} and Φ^-_{pksi}. The same for the binary variables q^+_{pks} and q^-_{pks} for the usage of the chargers. Finally, for reasons explained in subsection 3.7.3, the variables for monitoring the increased SOC are modified. They are indexed also over the time periods. So we have soc^+_{pdk} to model the quantity of SOC charged during period p along segment d in vehicle k and the analogous for u^+_{pdk}. Also these variables are included in Table A.2.

Note that, if there are no EVs provided with V2G technologies, the problem becomes the same of EEV-CSP (except for the variables used to model the degradation). Indeed, we add a constraint that restrict the bidirectional flow to EV-V2Gs (3.85). The binary variables q^-_{pks} allow the opposite flow of current, so if they are all set to zero, the discharging process in the model is neglected.

$$q^-_{pks} = 0 \qquad k \in \mathcal{K} \setminus \mathcal{H}, s \in \mathcal{S} \setminus \mathcal{T}, p \in \mathcal{P} \tag{3.85}$$

3.7.1 Revenue of the grid

V2G technologies are added to the contest in section 3.4 in order to decrease the power retrieved from the grid thanks to their peak-shaving effect. It is necessary then, to quantify the revenue attainable by the grid when the fleet is provided with such technologies. A practical way to estimate the grid revenue is detailed in Kempton and Tomić, 2005. In the paper it is stated that the power gained by the grid is limited by three factors. The first is the *power limited by the line*, which depends on the capacity of the wires and the circuits connecting to the grid. Then there is the *power limited by the vehicle's stored energy*, which depends on the power dispatched by the energy dispatched by the vehicle. The last is the *rated maximum power of the vehicle's power electronics*. The maximum power attainable as grid revenue corresponds to the lowest among the three. Kempton and Tomić (2005) explain also that typically the third quantity is much larger than the others. Furthermore, being a depot of a large public transportation service, it is reasonable to assume that the structure of the line itself is not limiting the grid. As a results, the grid revenue depends on the power limited by the vehicle's stored energy. Let this quantity be $P_{vehicle}$. It is now explained how to achieve a reasonable approximation of this value.

Kempton and Tomić, 2005 compute it as

$$P_{vehicle} = \frac{\left(E_s - \frac{d_d + d_{rb}}{\eta_{veh}}\right)}{t_{disp}} \cdot \eta_{inv} \tag{3.86}$$

where E_s is the maximum quantity of energy the vehicle could store, d_d is the distance driven since the energy storage was full, d_{rb} express the distance that the driver still want to be able to cover, η_{veh} is the vehicle driving efficiency and η_{inv} takes into account the conversion from DC to AC. This equation is not directly applicable to the situation of this problem, so it is necessary to understand the meaning of the quantity that it is trying to explain and adapt them to the contest. The numerator of Equation 3.86 is made up of three addends:

$$E_s - \frac{d_d}{\eta_{veh}} - \frac{d_{rb}}{\eta_{veh}} \tag{3.87}$$

which are the total capacity, the energy used so far and the energy to be used in the future. It basically measures the energy that the vehicle can give to the grid. In this situation, it directly corresponds to the one dispatched by the vehicle while discharging. This quantity must be related with the variation of SOC, but cannot be really computed from it. Indeed by rewriting the SOC definition (Equation 3.6) we have that

$$SOC(t + \delta) - SOC(t) = \frac{\int_t^{t+\delta} i\,dt}{Q} = \int_t^{t+\delta} \frac{i}{Q} dt \tag{3.88}$$

where the integral is the area above the curve of charging as shown in Figure 3.6 The
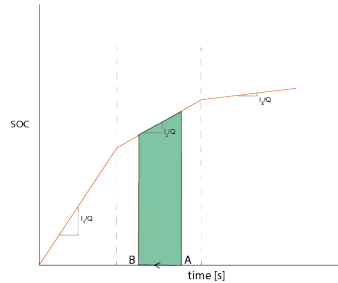
Figure 3.6: Relationship between SOC variation and dispatched power

area that we can compute has no dimensions, so it cannot be a power. Once again the results in Pelletier et al., 2018 are exploited by analogy. Indeed in the paper, starting from the battery model of Tremblay et al., 2007, some numerical simulation conducted on the CC-CV process showed that the cumulative energy recharged in a EV is linear with respect to the SOC. From this, the energy recharged in the battery is computed as the SOC variation by the energy capacity E. It follows

$$P_{vehicle} = \frac{E \cdot \Delta SOC}{\delta} \eta_{inv} \tag{3.89}$$

which is indeed a power [W]. Since Equation 3.89 computes the power dispatched by a vehicle, for the consideration made at the beginning of this chapter, the power retrieved from an EV-V2G by the grid is the opposite of it. Notice that since the

SOC of a vehicle decreases while discharging, the power obtained by the grid, being the opposite, is positive.

As the variables Φ^-_{pksi} are used for the decrease of SOC due to the discharging, they can be directly used in Equation 3.89. For coherence, the power requested from the grid for the charging, is no longer modified as the instantaneous power in constraint (3.68), but instead we consider the medium power which depends on energy used for charging. Finally, again from the relation between energy and power, we add the contribution of the power requested from the depot. The resulting constraint is reported in Equation 3.90.

$$\frac{\pi_p}{\delta} + \frac{E}{\delta} \left[\sum_{k \in \mathcal{K}} \sum_{s \in \mathcal{S}} \sum_{i \in B_s \setminus \{0\}} \left(\Phi^+_{pksi} - \eta_{inv} \Phi^-_{pksi} \right) \right] \leq y \qquad p \in \mathcal{P} \qquad (3.90)$$

3.7.2 Load valley effect

Another important aspect of V2G-technologies is their load valley filling. With this term we refer to the possibility of exploiting such technologies to buy energy at cheaper prices and use it during high-cost periods. Namely, since in this setting energy prices vary with periods, an EV could be charged during a low cost period and discharged at a high cost period. In this way the grid would be able to exploit energy bought at a discounted price. Note that, because of inefficiency in the flow of current from the vehicle to the grid, a factor of η_{inv} of energy will be lost during the process. The energy discharged by EV-V2Gs can also be beneficial for the depot itself as it may help or satisfy the depot demand.

To integrate V2Gs in the model, we modify the objective function. In particular, we have a revenue every time we used energy from other vehicles. The contribution for the energy costs becomes

$$\sum_{p \in P} c_p \left(\pi_p + E \sum_{k \in K} \sum_{s \in \mathcal{S}} \sum_{i \in B_s \setminus \{0\}} \left(\Phi^+_{pksi} - \eta_{inv} \Phi^-_{pksi} \right) \right), \qquad (3.91)$$

where indeed we have the depot demand, the energy used for charging and a discount for the discharged energy weighed by η_{inv}. Notice that the cost in Equation 3.91 related to the depot demand is a sort of a fixed cost: we always have to buy energy for a cost of $c_p \cdot \pi_p$, but if some EV-V2G discharges some energy, than we will have a reduction on it.

We report here also the modifications due to the charging process. As already remarked the discharging process is modeled according to the CC-CV curve as well. So, to integrate it in the model, it is enough to adapt Equation 3.46 and Equation 3.45, as in (3.92) and (3.93). Constraints (3.47) are extended to discharge in Equation 3.94. The same reasoning of EEV-CSP is applied to the usage of the chargers for the discharging process (3.95) and (3.96).

$$SOC_{pk} - \sum_{i' \geq i} \Phi^-_{pksi'} \geq a_{s,i-1} x^-_{pksi} + SOC_{min} \left(1 - x^-_{pksi} \right) \qquad (3.92)$$

$$p \in \mathcal{P}, k \in \mathcal{K}, s \in \mathcal{S}, i \in B_s \setminus \{0\}$$

$$SOC_{pk} - \sum_{i'>i} \Phi^-_{pksi'} \leq a_{si}x^-_{pksi} + SOC_{max}\left(1 - x^+_{pksi}\right) \tag{3.93}$$

$$p \in \mathcal{P}, k \in \mathcal{K}, s \in \mathcal{S}, i \in B_s \setminus \{0\}$$

$$\Phi^-_{pksi} \leq (a_{si} - a_{s,i-1})x^-_{pksi} \qquad p \in \mathcal{P}, k \in \mathcal{K}, s \in \mathcal{S}, i \in B_s \setminus \{0\} \tag{3.94}$$

$$q^-_{pks} \leq \sum_{i \in B_s \setminus \{0\}} x^-_{pksi} \qquad p \in \mathcal{P}, k \in \mathcal{K}, s \in \mathcal{S} \tag{3.95}$$

$$q^-_{pks} \geq x^-_{pksi} \qquad p \in \mathcal{P}, k \in \mathcal{K}, s \in \mathcal{S}, i \in B_s \setminus \{0\} \tag{3.96}$$

Finally, the SOC update (3.49) of EV-V2Gs needs to take into account also the loss of SOC due to the discharging process. Note that in Equation 3.97 the variables Φ^-_{pksi} are not discounted by η_{inv}, as the dissipation happens when the energy returns to the grid.

$$SOC_{p+1,k} = SOC_{pk} + \sum_{s \in \mathcal{S}} \sum_{i \in B_s \setminus \{0\}} \left(\Phi^+_{pksi} - \Phi^-_{pksi}\right) \qquad p \in \mathcal{P} \setminus \{n_p\}, k \in \mathcal{K} \tag{3.97}$$

3.7.3   Degradation costs for the V2G setting

When introducing V2G technologies, the charging and discharging process of the batteries could become more frequent. This would lead to a higher impact on the degradation costs. In this section it is explained how the wear cost function presented in section 3.1 is adapted to the V2G scenario.

In the last section of the paper, Han et al., 2014 propose also a model to compute degradation costs when employing V2G technologies. In particular they show its application on their previous model in S. Han et al. (2012). For sake of a better comprehension of the application, this problem will be quickly resumed.

In the setting in S. Han et al. (2012), a house is equipped with a solar photovoltaic system (PV). An electric vehicle provided with V2G technologies with initial SOC_{init} is connected to the grid until time T. The control model aims at understanding the power r_i that must be used to charge the vehicle guaranteeing the requested state of charge at time T, namely in a range $SOC_{TL} - SOC_{TU}$. V2G technologies are used for their ancillary services, in particular for the regulation. The agent has a reward both for the regulation up (P_{RUi}) and the regulation down (P_{RDi}). These to are also weighted according to W_{RD} and W_{RU}. Regulation services can be apply up to a maximum value charge C and discharge D power. The profile of the expected energy load for the house in every period is known E_i along with the expected amount of PV generation G_i. A control problem is then modeled to understand the average charging power r_i for the vehicle. Power can be bought or sell with a reward of P_{ep}. The state of charge s_i is used as a proxy variable in every period i. The control model is as follows.

$$\arg max_{r_i} \sum_{i=1}^{N}(W_{RD}(s_i)P_{RD_i}(C - r_i) + W_{RU}(s_i)P_{RU_i}(D + r_i)) \tag{3.98}$$
$$+ P_{ep}(E_i + r_i - G_i)$$

$$\text{s.t.} \qquad SOC_{TL} \leq s_N \leq SOC_{TU} \tag{3.99}$$

$$s_{i+1} = s_i + \frac{r_i}{Q} \qquad i = 1 \ldots N \tag{3.100}$$

$$-D \leq r_i \leq C \qquad i = 1 \ldots N \tag{3.101}$$

$$s_0 = SOC_{init} \tag{3.102}$$

The control variable for the charging current r_i typically is constant for periods which last even a hour and are indexed on i. Regulation instead varies more frequently, just after seconds. When considering the degradation costs for V2G vehicles, the authors model a new variable for the power $p_{i,j}$ defined as

$$p_{i,j} = r_i + v_j, \qquad j \in T_i \tag{3.103}$$

where v_j is the regulation power which varies over few seconds. Seconds are indexed on j and T_j is indeed the time set for regulation at the i-th period. Let t be the length of the period indexed in i. With this new definition of power $p_{i,j}$, degradation costs are computed as follows.

$$WearCost_{ij} = W(\mathbb{E}\left[s_{ij}\right])_d \Delta Q_{ij} \tag{3.104}$$

where

$$\mathbb{E}\left[s_{ij}\right] = \bar{s}_{ij} + \frac{1}{2}\frac{\mathbb{E}\left[p_{ij}\right]t}{BatterySize} \tag{3.105}$$

$$\Delta Q_{i,j} = \mathbb{E}\left[|p_{ij}|\right]t \tag{3.106}$$

Then the authors develop these terms. In particular they obtain equations that depend on the power r_i rather than the state of charge. However since the models in this work have a direct control on the state of charge of the batteries by means of the variables SOC_{pk}, there is no need to go further and it is just sufficient to interpret equations (3.104) - (3.106) and adapt them to the context. In particular it can be noticed that:

- the wear cost function is the same as the one fitted for the vehicles without V2G from Equation 3.3

- such function must be evaluated in the SOC of the period we are considering

- both the absolute value of outgoing and incoming energy must be taken into account when computing Δq

In analogy with Equation 3.106, all the contributions must be considered with their absolute value. Basically this means that the area represented by Equation 3.12 is computed following every step the trajectory of the SOC. Since we are assuming that the final and the initial SOC are equal, we can consider the contributions only along one direction and double the wear cost parameters w_d. We model the increase of SOC and Equation 3.12 is modelled as

$$\sum_{d \in \mathcal{D}} soc^+_{pdk} = \sum_{s \in \mathcal{S}} \sum_{i \in B_s \setminus \{0\}} \Phi^+_{pksi} \qquad p \in \mathcal{P}, k \in \mathcal{K}, \tag{3.107}$$

so that all the increase of SOC are accounted.

Notice that Equation 3.107 considers only the total variation of SOC, but then this value needs to be divided into the proper interval $\mathcal{D}$. To do this, being now the model really complex, we do not rely anymore on the monotonicity of the wear cost function but instead we use an exact approach. We model this following the same idea of the charging process in EEV-CSP. Indeed, for every segment we have an amount of SOC charged and a binary variable that tells whether that segment is used or not. So, to split the model, the part of the degradation of battery needs to be modified as in (3.108) - (3.110).

$$soc_{pdk}^+ \leq L u_{pdk}^+ \quad d \in \mathcal{D}, k \in \mathcal{K}, p \in \mathcal{P} \tag{3.108}$$

$$SOC_{pk} + \sum_{d'<d} soc_{pd'k}^+ \geq \bar{\delta}_{d-1} u_{pdk}^+ + SOC_{min}\left(1 - u_{pdk}^+\right) \qquad p \in \mathcal{P}, d \in \mathcal{D}, k \in \mathcal{K}, p \notin A_k \tag{3.109}$$

$$SOC_{pk} + \sum_{d'\leq d} soc_{pd'k}^+ \leq \bar{\delta}_d u_{pdk}^+ + SOC_{max}\left(1 - u_{pdk}^+\right) \qquad p \in \mathcal{P}, d \in \mathcal{D}, k \in \mathcal{K}, p \notin A_k \tag{3.110}$$

We report now the MILP formulation of the EEV-CSP-V2G.

$$\min \sum_{p\in P} c_p \left(\pi_p + E \sum_{k\in K}\sum_{s\in\mathcal{S}}\sum_{i\in B_s\backslash\{0\}} \left(\Phi_{pksi}^+ - \eta_{inv}\Phi_{pksi}^-\right)\right) + F \cdot y+ \tag{3.111}$$

$$2w_d E \sum_{d\in\mathcal{D}}\sum_{k\in\mathcal{K}}\sum_{p\in\mathcal{P}} soc_{pdk}^+$$

s.t. $$q_{pks}^- = 0 \qquad k \in \mathcal{K}\setminus\mathcal{H}, s \in \mathcal{S}\setminus\mathcal{T}, p \in \mathcal{P} \tag{3.112}$$

$$\pi_p + E \cdot \left(\sum_{k\in\mathcal{K}}\sum_{s\in\mathcal{S}}\sum_{i\in B_s\backslash\{0\}} \Phi_{pksi}^+ - \eta_{inv}\sum_{k\in\mathcal{K}}\sum_{s\in\mathcal{S}}\sum_{i\in B_s\backslash\{0\}} \Phi_{pksi}^-\right) \geq 0 \qquad p \in \mathcal{P} \tag{3.113}$$

$$\sum_{p=\beta_r}^{\alpha_r}\sum_{s\in\mathcal{S}} \left(q_{pv_r s}^+ + q_{pv_r s}^-\right) = 0 \qquad r \in \mathcal{R} \tag{3.114}$$

$$\sum_{k\in K} \left(q_{pks}^+ + q_{pks}^-\right) \leq \kappa_s \qquad p \in \mathcal{P}, s \in \mathcal{S} \tag{3.115}$$

$$\sum_{s\in S} \left(q_{pks}^+ + q_{pks}^-\right) \leq 1 \qquad p \in \mathcal{P}, k \in \mathcal{K} \tag{3.116}$$

$$q_{pks}^+ \leq \sum_{i\in B_s\backslash\{0\}} x_{pksi}^+ \qquad p \in \mathcal{P}, k \in \mathcal{K}, s \in \mathcal{S} \tag{3.117}$$

$$q_{pks}^+ \geq x_{pksi}^+ \qquad p \in \mathcal{P}, k \in \mathcal{K}, s \in \mathcal{S}, i \in B_s \setminus \{0\} \tag{3.118}$$

$$q_{pks}^- \leq \sum_{i\in B_s\backslash\{0\}} x_{pksi}^- \qquad p \in \mathcal{P}, k \in \mathcal{K}, s \in \mathcal{S} \tag{3.119}$$

$$q_{pks}^- \geq x_{pksi}^- \qquad p \in \mathcal{P}, k \in \mathcal{K}, s \in \mathcal{S}, i \in B_s \setminus \{0\} \tag{3.120}$$

$$SOC_{\alpha_r,k_r} = SOC_{\beta_r,k_r} - \Delta SOC_r \qquad r \in \mathcal{R} \tag{3.121}$$

$$SOC_{pk} + \sum_{i' \leq i} \Phi^+_{pksi'} \leq a_{si} x^+_{pksi} + SOC_{max} \left(1 - x^+_{pksi}\right) \tag{3.122}$$

$$p \in \mathcal{P}, k \in \mathcal{K}, s \in \mathcal{S}, i \in B_s \setminus \{0\}$$

$$SOC_{pk} + \sum_{i' < i} \Phi^+_{pksi'} \geq a_{s,i-1} x^+_{pksi} + SOC_{min} \left(1 - x^+_{pksi}\right) \tag{3.123}$$

$$p \in \mathcal{P}, k \in \mathcal{K}, s \in \mathcal{S}, i \in B_s \setminus \{0\}$$

$$SOC_{pk} - \sum_{i' \geq i} \Phi^-_{pksi'} \geq a_{s,i-1} x^-_{pksi} + SOC_{min} \left(1 - x^-_{pksi}\right) \tag{3.124}$$

$$p \in \mathcal{P}, k \in \mathcal{K}, s \in \mathcal{S}, i \in B_s \setminus \{0\}$$

$$SOC_{pk} - \sum_{i' > i} \Phi^-_{pksi'} \leq a_{si} x^-_{pksi} + SOC_{max} \left(1 - x^+_{pksi}\right) \tag{3.125}$$

$$p \in \mathcal{P}, k \in \mathcal{K}, s \in \mathcal{S}, i \in B_s \setminus \{0\}$$

$$\Phi^+_{pksi} \leq (a_{si} - a_{s,i-1}) x^+_{pksi} \qquad p \in \mathcal{P}, k \in \mathcal{K}, s \in \mathcal{S}, i \in B_s \setminus \{0\} \tag{3.126}$$

$$\Phi^-_{pksi} \leq (a_{si} - a_{s,i-1}) x^-_{pksi} \qquad p \in \mathcal{P}, k \in \mathcal{K}, s \in \mathcal{S}, i \in B_s \setminus \{0\} \tag{3.127}$$

$$SOC_{p+1,k} = SOC_{pk} + \sum_{s \in \mathcal{S}} \sum_{i \in B_s \setminus \{0\}} \left(\Phi^+_{pksi} - \Phi^-_{pksi}\right) \qquad p \in \mathcal{P} \setminus \{n_p\}, k \in \mathcal{K} \tag{3.128}$$

$$SOC_{1k} = SOC_{n_pk} + \sum_{s \in \mathcal{S}} \sum_{i \in B_s \setminus \{0\}} \left(\Phi^+_{n_pksi} - \Phi^-_{n_pksi}\right) \qquad k \in \mathcal{K} \tag{3.129}$$

$$\sum_{s \in \mathcal{S}} \sum_{i \in B_s \setminus \{0\}} \frac{\Phi^+_{pksi} + \Phi^-_{pksi}}{I_{si}} Q \leq \delta \qquad p \in \mathcal{P}, k \in \mathcal{K} \tag{3.130}$$

$$SOC_{min} \leq SOC_{pk} \leq SOC_{max} \qquad p \in \mathcal{P}, k \in \mathcal{K} \tag{3.131}$$

$$\frac{\pi_p}{\delta} + \frac{E}{\delta} \left[\sum_{k \in \mathcal{K}} \sum_{s \in \mathcal{S}} \sum_{i \in B_s \setminus \{0\}} \left(\Phi^+_{pksi} - \eta_{inv} \Phi^-_{pksi}\right) \right] \leq y \qquad p \in \mathcal{P} \tag{3.132}$$

$$0 \leq y \leq G \tag{3.133}$$

$$z_{1k} \geq q^+_{1ks} - q^+_{n_pks} \qquad k \in \mathcal{K}, s \in \mathcal{S} \tag{3.134}$$

$$z_{pk} \geq q^+_{pks} - q^+_{p-1,ks} \qquad p \in \mathcal{P} \setminus \{1\}, k \in \mathcal{K}, s \in \mathcal{S} \tag{3.135}$$

$$z_{pk} \geq q^-_{pks} - q^-_{p-1,ks} \qquad p \in \mathcal{P} \setminus \{1\}, k \in \mathcal{K}, s \in \mathcal{S} \tag{3.136}$$

$$z_{1k} \geq q^-_{1ks} - q^-_{n_pks} \qquad k \in \mathcal{K}, s \in \mathcal{S} \tag{3.137}$$

$$\sum_{p=\alpha_{\eta_r}}^{\beta_r - 1} z_{pv_r} \leq C \qquad r \in \mathcal{R} \setminus \{f_k | k \in \mathcal{K}\} \tag{3.138}$$

$$\sum_{p=\alpha_{l_k}}^{\beta_{f_k} - 1} z_{pk} \leq C \qquad k \in \mathcal{K} \tag{3.139}$$

$$\sum_{d \in \mathcal{D}} soc^+_{pdk} = \sum_{s \in \mathcal{S}} \sum_{i \in B_s \setminus \{0\}} \Phi^+_{pksi} \qquad p \in \mathcal{P}, k \in \mathcal{K} \tag{3.140}$$

$$soc^+_{pdk} \leq L u^+_{pdk} \qquad d \in \mathcal{D}, k \in \mathcal{K}, p \in \mathcal{P} \tag{3.141}$$

$$SOC_{pk} + \sum_{d' < d} soc^+_{pd'k} \geq \overline{\delta}_{d-1} u^+_{pdk} + SOC_{min}\left(1 - u^+_{pdk}\right) \tag{3.142}$$

$$p \in \mathcal{P}, d \in \mathcal{D}, k \in \mathcal{K}, p \notin A_k$$

$$SOC_{pk} + \sum_{d' \leq d} soc^+_{pd'k} \leq \overline{\delta}_d u^+_{pdk} + SOC_{max}\left(1 - u^+_{pdk}\right) \tag{3.143}$$

$$p \in \mathcal{P}, d \in \mathcal{D}, k \in \mathcal{K}, p \notin A_k$$

$$0 \leq SOC_{pk} \leq 1 \qquad p \in \mathcal{P}, k \in \mathcal{K} \tag{3.144}$$

$$x^+_{pksi} \in \{0, 1\} \qquad p \in \mathcal{P}, k \in \mathcal{K}, s \in \mathcal{S}, i \in B_s \setminus \{0\} \tag{3.145}$$

$$x^-_{pksi} \in \{0, 1\} \qquad p \in \mathcal{P}, k \in \mathcal{K}, s \in \mathcal{S}, i \in B_s \setminus \{0\} \tag{3.146}$$

$$q^+_{pks} \in \{0, 1\} \qquad p \in \mathcal{P}, k \in \mathcal{K}, s \in \mathcal{S} \tag{3.147}$$

$$q^-_{pks} \in \{0, 1\} \qquad p \in \mathcal{P}, k \in \mathcal{K}, s \in \mathcal{S} \tag{3.148}$$

$$\Phi^+_{pksi} \geq 0 \qquad p \in \mathcal{P}, k \in \mathcal{K}, s \in \mathcal{S}, i \in B_s \setminus \{0\} \tag{3.149}$$

$$\Phi^-_{pksi} \geq 0 \qquad p \in \mathcal{P}, k \in \mathcal{K}, s \in \mathcal{S}, i \in B_s \setminus \{0\} \tag{3.150}$$

$$y \geq 0 \tag{3.151}$$

$$z_{pk} \in \{0, 1\} \qquad p \in \mathcal{P}, k \in \mathcal{K} \tag{3.152}$$

$$soc^+_{pdk} \geq 0 \qquad p \in \mathcal{P} \setminus \{1\}, d \in \mathcal{D}, k \in \mathcal{K} \tag{3.153}$$

$$u^+_{pdk} \in \{0, 1\} \qquad p \in \mathcal{P} \setminus \{1\}, d \in \mathcal{D}, k \in \mathcal{K} \tag{3.154}$$

Each one of the panels in Figure 3.7 represents a schedule of the fleet. Every line is associated with an EB. Blue bars are for the routes. The usage of a charger is represented by the green bars when charging and by red bars when discharging. In particular, if the a bar is dark green it means that we the vehicle is using a fast charger, while light green bars are for slow chargers. At the same time, dark red bars are used whenever an EV-V2G is discharging energy by means of a fast charger and light red when instead a slow charger is used. In Figure 3.7 we compare three charge schedules obtained with the three models discussed. In particular, we notice that in the one of EV-CSP (3.7a), all EVs are fully charged at the beginning of the time horizon while their SOC is really low at the end of the period. Then, 3.7b shows the schedule obtained according to EEV-CSP, while 3.7c is for EEV-CSP-V2G. Notice that, even if V2Gs are not used in 3.7c, the schedule is different from the one of EEV-CSP as it is indeed a different model.

3.8   A heuristic for the EEV-CSP-V2G

As it will be analyzed in details in the chapter 5, the solution of EEV-CPS-V2G is rather difficult for medium-sized instances. Therefore, in order to have a solution method able to tackle a real problem, we developed an heuristic We note that it is not straightforward the reasons behind the complexity of resolution the model.

We have attempted to developed and tried several matheuristics to solve the problem. We tried to remove the grid restriction and the maximum power retrieved. Indeed, when optimizing the variable y, we are trying to solve a min-max problem which can make the process really difficult for the solver. Once obtained the solution of this first step is obtained, we computed how much it was charged in every cost

(a) Charge scheduling with EV-CSP model

(b) Charge scheduling with EEV-CSP model

(c) Charge scheduling with EEV-CPS-V2G model

Figure 3.7: Comparison of the charge scheduling obtained according to the different models

period. We tried to use this information to guide the solution of the whole problem. Unfortunately, this procedure has not been effective. In particular, even removing the constraints related with the y variable the derived problem was still hard to be solved.

We decided then to focus on other coupling constraints. As the constraints related with y do not change the complexity of the model, we decided to remove the constraints on the number of chargers (3.115). We substituted them with a soft version. Given the number of chargers available in the depot, we computed the mean of the SOC that EBs can charged. In the new constraint, we ensured that the total SOC charged is less or equal than the estimated value. Then we optimized the problem. The solution of this problem is really fast. However, typically the number of chargers used exceeds the available ones, leading to infeasible solutions. To overcome this issue, we developed a second step to obtain a feasible solution. Again, for every cost period we computed the amount of energy charged and use it in the second step. However, this second problem proved to be really hard to be solved and also this heuristic was not effective.

Given the difficulties in the improvement of the second step, instead of removing or substituting constraints, we decided to solve the problem with a restricted objective function. In this way indeed, even if a further second step is not able to find an optimal solution, the one found in the first step is a solution for the whole problem, even if sub optimal. We analyzed the solution for different sub problems, optimizing each time only a subset of the objective function. All the results obtained for the subproblems are reported in chapter 5. In general, we have different situations depending on the sub-problem we are solving. The optimization of the degradation costs seems to increase the complexity of the model. On the other hand, when optimizing only the energy component, the FRD costs or these two together, the solver is always able to provide a solution within the time limit. In particular, the optimization of energy and FRD costs jointly, produces a good quality solution for all the instances and takes into account the two major components of the costs. Therefore, the resolution of this sub-problem is exploited to find a feasible solution for the EEV-CSP-V2G. As second step, we tried first to use the solver with a cutoff. Since it was not effective, we used instead a warm-up. This last heuristic has proved to be beneficial. Thus, our heuristic is made of two steps that we summarized here:

- The model is solved optimizing energy and FRD costs

- The solution found in step 1 is passed to the solver as MIP start and the complete model is solved

In chapter 5 we show the application of such heuristic on a variety of experiments.

Chapter 4

Case study

The base case instances are inspired from the public transportation system of the city of Milan (ATM). As stated in the communication "*ATM: DAL 2030 FULL ELECTRIC*" on ATM website, a fleet of exclusively EBs will be available by 2030. ATM announced that each of the 12 meter EBs will be equipped with a 240kWh lithium-phosphate battery, allowing an autonomy of almost 180 km. As a consequence, the battery charge capacity will be of 120 Ah. The specific characteristics of the batteries of EBs are not known, so several assumptions are made on the base of the studies on the EBs fleet in *New Energy Outlook 2020* and S. Pelletier, Jabali, Mendoza, et al., 2019.

We assume that two types of chargers are available at the depot, slow and fast chargers. The former have a power of 80kW and are able to fully charge an EB in 5 hours (4.1a). The latter are of 120 kW and the complete charge takes less then 4 hours (4.1a). The number of the charger facilities depends on the fleet itself in the ratio of 1:2 and 1:3 respectively. For both chargers a CC-CV curve is approximated by means of the following piece-wise linear approximations (Figure 4.1).

To estimate the wear cost function, it is necessary to know the initial price of batteries. In *New Energy Outlook 2020* report, the trend of battery prices is explained. The initial price of batteries is subjected to a great variability depending on the year. In particular, it decreases over years. Given the time horizon of this work, with a plan of conversion of the fleet from 2020 to 2030, a price of 81,79 €/kWh is a reasonable estimate. The wear cost function w_d is then fitted according to the procedure described in section 3.3 using a set of 4 equidistant points. It follows that $|\mathcal{D}|= 4$, with $L = 0.25$. The interval for the SOC calibration as well as the values of the wear cost function are reported in Table 4.1.

We assume that the depot is under an industrial energy contract that simulates the "Enel Energy Placet Fix" plan for commercial users (ROSSETTI, 2020). The time dependent energy prices c_p have 3 different values with a peak period from 8.00 to 19.00. Low energy prices are available during the night from 23.00 to 7.00, while in all the other periods energy has an intermediate cost. The FRD cost F is equal to 144 €/kW every year. Assuming 20 working day per month, it is equivalent to 0.6€/kW for a daily planning horizon. These costs are summarized in Table 4.2.

The maximum load supported by the grid is not specified in the contract. Usually indeed the grid capacity depends on its employment. To approximate this value, we have computed the biggest load that could be required to the grid, which
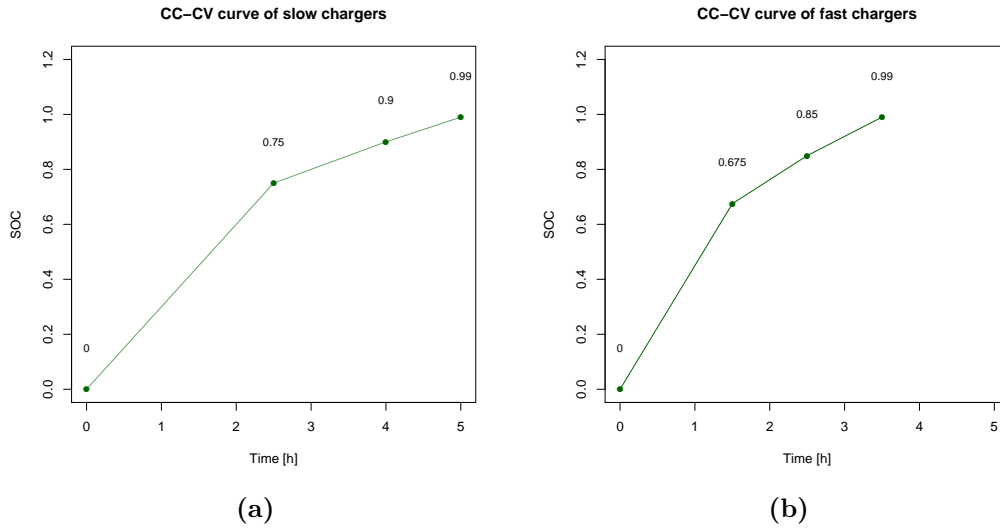
Figure 4.1: CC-CV curve of a slow and a fast charger

SOC interval	Degradation costs
0-0.25	€0.10/kWh
0.25-0.50	€0.10/kWh
0.50-0.75	€0.12/kWh
0.75-1.0	€0.16/kWh

Table 4.1: Battery wear cost function

is obtained when the depot demand is maximal and all the chargers are used with maximum power. The grid capacity parameter G is then 80% of the this worst case scenario.

As already discussed, we have introduced also a demand profile of the depot. In this scenario, this is obtained with a perturbation of the profile energy of a non refrigerated warehouse in Washington US in 2016-2017. Due to privacy reasons we cannot disclose the source of this data.

Data are cyclic with respect to the year and seasonal along with seasons. Furthermore there is a daily variation in the demand. From the average hourly energy demand during working days the following profiles for summer and winter are obtained.

Period	Cost
Peak (8.00-19.00)	0.111
Mid (7.00-8.00, 19.00-23.00)	0.108
Off-peak (23.00-7.00)	0.095
FRD charges	144

Table 4.2: Rates (€/kWh) and yearly FRD charge (€/kW)
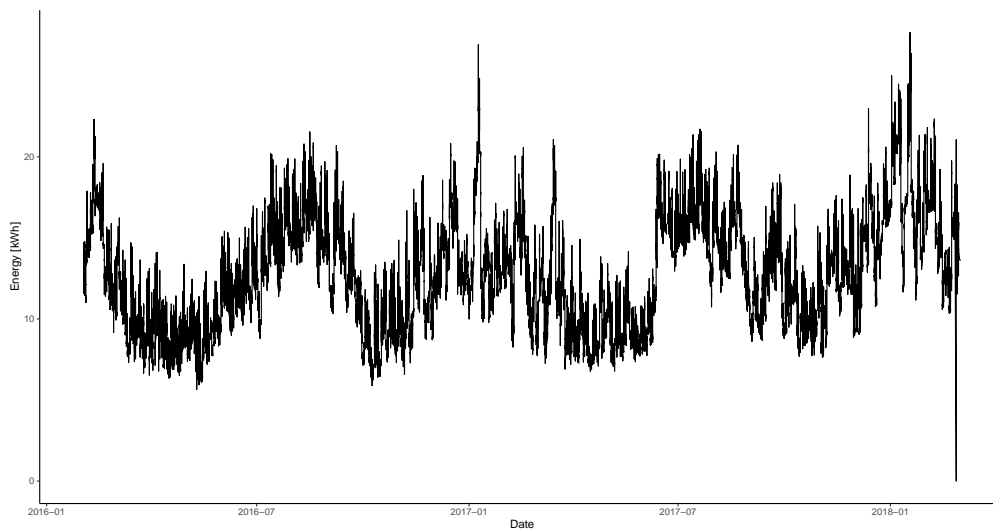
Figure 4.2: Depot demand over 2016-2017
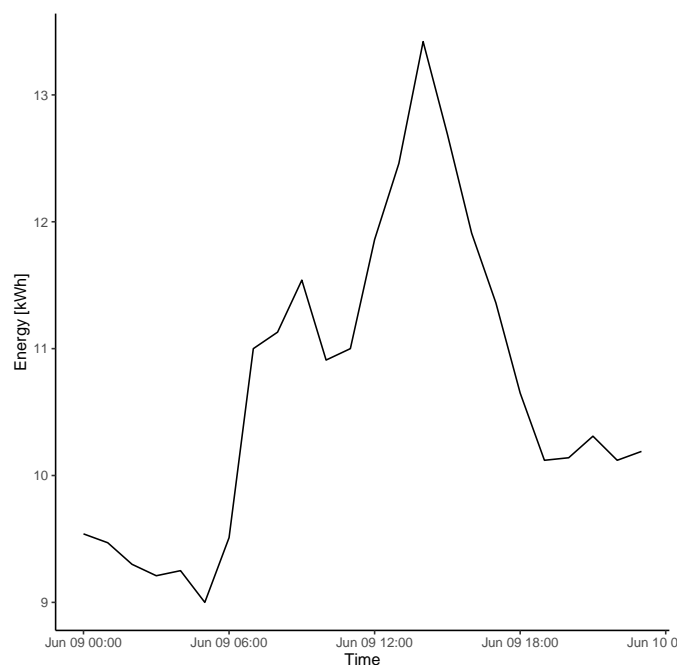
Figure 4.3: Depot energy profile of a random day

The planning horizon is of one day and it is divided into periods of 30 minutes. Additional assumptions are that between routes it is possible to plug in an EB only three times and their SOC needs to be in the range [0.05 0.99].

4.0.1 Instances

The routes planning is based on the fleet of buses of ATM. Data are available on ATM website (di Milano, n.d.(a)-di Milano, n.d.(b)). Lines *44 50 54 56 57 59 60 73 74 80 88 89 95 121* of ATM service have been considered. The frequencies of buses are available from ATM timetables (4.5).
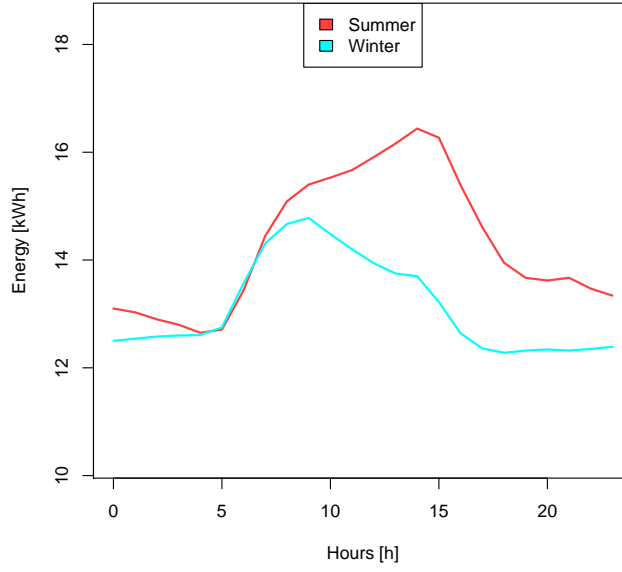
Figure 4.4: Distribution of depot demand according to the season and mean depot demand in a day

Figure 4.5: Example of an ATM time table for a bus line

Furthermore, the travel time for a journey is different according to the day time. The hourly travel time is the mean of the values reported at differen hours on *GoogleMaps*. With these data, a simple model to estimate the SOC consumption of an EB that leaves the depot at time t_1 and returns at time t_2 is developed as follows:

$$\Delta SOC_{t_1, t_2} = \eta_{conv} \cdot SeasonFactor \cdot \sum_{t=t_1}^{t_2} (0.95 \cdot MeanDistance(t) \cdot \Delta t) \quad (4.1)$$

where η_{conv} is the energy consumption per kilometers (0.99), season factor is a value that takes into account the different consumption in during winter (1.14) and summer (1.09). Finally, $MeanDistance(t)$ is a function that returns the mean distance of the considered bus at time t. According to (4.1), the average SOC consumption relies only on the departure and arrival at the depot. Therefore, in order to simulate the instances it is just necessary to simulate the departure and arrival of every route and then compute the SOC consumption on their base. With such route planning, we try to capture the behavior of the fleet during the day as described on ATM Website.

Peak hours are at (7.00-9.00) and mid-peak hours (17.00-20.00). Also in the night bus frequencies decrease a lot. The service starts at 5.00 and ends around 1.00. To simulate this behaviour, all the EBs are forced to leave the depot in the morning at a period that is sampled between 5.00 and 7.00, with a probability given by the frequencies of the data set. After the peak time, an EB may come back at the depot. Based on the frequencies in data-set, the event "EB returns at the depot" is distributed as a Bernoulli variable of parameter 0.3, $Be(0.3)$. This means that one third of the fleet is expected to come back in the depot. The return time at the depot after peak hours is randomly generated as a uniform from 10.00 to 12.00. A second route is assigned to these vehicles, which are forced to get outside again for the second peak of the fleet, again uniformly between 16.00 and 17.00. At night, EBs come back in the depot starting from 20.30 up until 1.30 according to the frequencies of the dataset. Furthermore, in order to ensure feasibility of the routes, some breaks at the depot are randomly added for the vehicles which are suppose to perform an initial route requiring more that 100% of the SOC. Instances are simulated for fleet of 10, 20, 30, 40, 50, 60, 70, 80, 90, 100 vehicles. Five instances are generated for each configuration. In figure 4.6 we show the route planning for some of these instances.
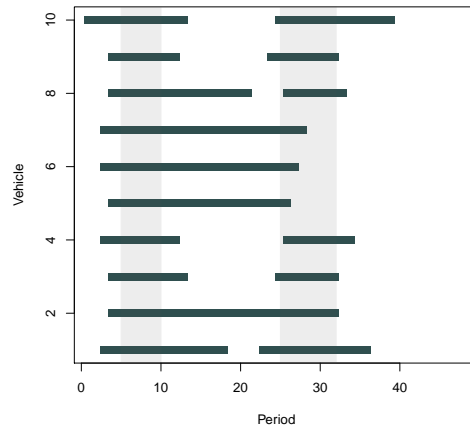
(a) 10 EBs
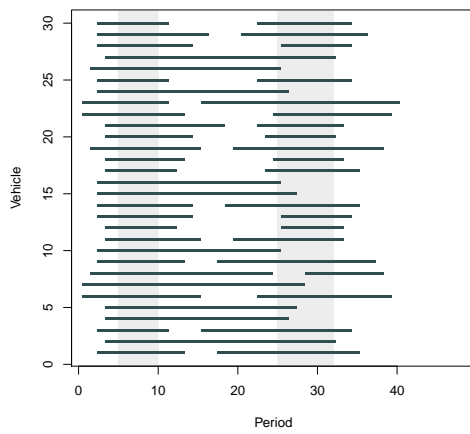
(b) 30 EBs
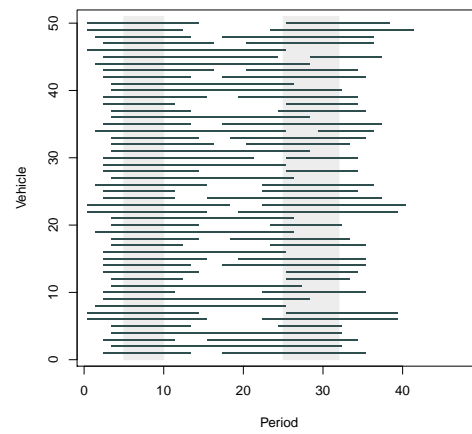
(c) 50 EBs
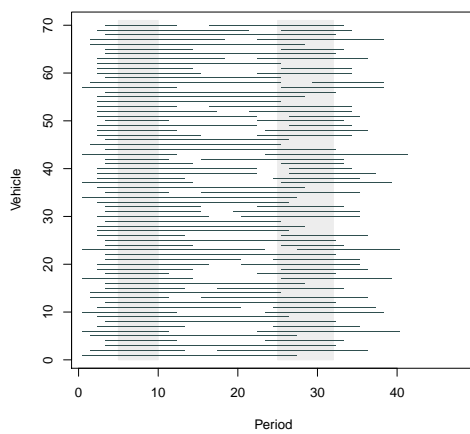
(d) 70 EBs
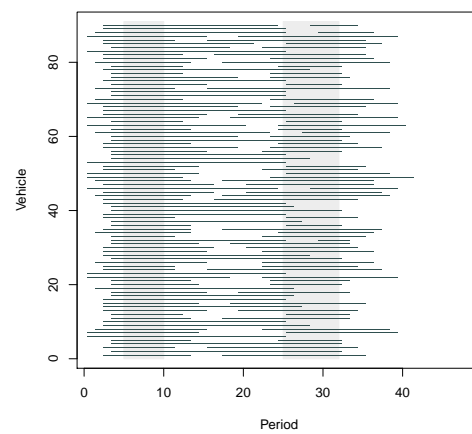
(e) 90 EBs

Figure 4.6: Some examples of the route scheduling for the fleets

Chapter 5

Computational experiments

A computational analysis on the scenario of chapter 4 has been performed to understand the complexity of the problem as well as investigating the employment of V2G technologies in the charge scheduling. The EEV-CPS-V2G model is implemented in C++ using the calleble library of the solver CPLEX 12.10. All the instances were solved up to an optimality GAP of 0.1%.

5.1 Base case results

The results of the EEV-CPS-V2G are presented in Table 5.1. Instances are denoted according to the fleet size. For example, "10_3" refers to the third instance among the ones with a fleet of 10 EBs. Each instance was run with a time limit of 2 hours. Whenever the solver is able to find a solution, all the partial contributions are reported as well as the total. Furthermore we report the GAP optimality and the time it took to find the solution. When the solver was not able to find a solution, the line is blank (except for the time limit). All the costs in the tables are in €, while the time is in seconds (s).

In Table 5.1 we report the results obtained when the EEV-CPS-V2G is solved to optimality. We have reported instances up to 30 EBs only since no solutions are found for larger fleets. Notice that neither for the smallest instances, the problem

	Energy	FRD	Deg	Total	GAP	Time
10_1	263.72	75.58	192.52	531.82	1.59%	7200
10_2	283.42	79.76	208.45	571.62	1.15%	7200
10_3	292.76	80.85	220.77	594.38	1.44%	7200
10_4	281.64	78.59	219.24	579.46	2.82%	7200
10_5	261.90	71.98	187.49	521.37	1.49%	7200
20_1	478.86	139.05	413.18	1031.09	2.32%	7200
20_2	492.10	139.59	425.44	1057.13	2.25%	7200
20_3						7200
20_4	469.99	133.17	396.87	1000.03	1.59%	7200
20_5	466.19	130.68	395.05	991.91	1.98%	7200
30_1						7200
30_2	688.50	194.56	625.58	1508.64	2.39%	7200
30_3						7200
30_4						7200
30_5						7200

Table 5.1: Optimization of EEV-CPS-V2G in the base case scenario

Fleet size	Average cost	Average GAP	Average Time	Optimal	Found solution
10	828.39	0.06%	14.70	5	5
20	1488.89	0.05%	61.81	5	5
30	2097.45	0.08%	185.19	5	5
40	2820.93	0.06%	320.22	5	5
50	3387.92	0.07%	1020.40	5	5
60	4068.60	0.05%	2546.17	5	5
70	4661.44	0.06%	3459.09	3	4
80	5254.60	0.09%	4566.41	3	3
90	5993.99	0.04%	5370.28	3	3
100	6543.18	0.05%	5518.72	4	4

Table 5.2: Summary of the results obtained optimizing only the energy costs. For the detailed results check Table 5.6

Fleet size	Average cost	Average GAP	Average Time	Optimal	Found solution
10	560.97	0.02%	10.41	5	5
20	1035.92	0.00%	38.34	5	5
30	1494.12	0.00%	76.39	5	5
40	2005.84	0.00%	144.14	5	5
50	2472.80	0.02%	173.32	5	5
60	2954.03	0.00%	296.55	5	5
70	3413.35	0.00%	312.95	5	5
80	3889.29	0.00%	350.78	5	5
90	4372.66	0.00%	399.93	5	5
100	4831.50	0.00%	489.78	5	5

Table 5.3: Summary of the results obtained optimizing FRD costs. For the detailed results check Table 5.7

is not solved up to optimality and we always reach the time limit.

These results show the necessity of a heuristic approach to solve the problem. As we have already explained in section 3.8 when we have introduced our heuristic, the first step of our strategy relies on the solution of the EEV-CPS-V2G , but with a subset of its objective function. We report here the different results obtained when we optimize these subproblems. Instances are solved optimizing only the degradation costs (Table 5.5), the energy costs (Table 5.6), the FRD costs (Table 5.7) or a combination of energy and FRD (Table 5.8).

In the instances where we optimize only the degradation costs (Table 5.5), we obtain poor results. No instances are solved up to optimality and the average GAP is 4.42% and the time limit is always reached.

As the other tables report the results for all the instances, we summarize them. In particular, for every fleet size, we report the average total costs, the average GAP and the average time to get a solution. Furthermore, we report the column "Optimal" that says how many instances are solved within our gap of optimality and "Found solution" to report the number of instances for which the solver is able to find a solution.

The solutions in which we optimized only the energy costs (5.6) are summarized in Table 5.2. Notice that out of the five instances for each category, when the fleet size is smaller than 50 EBs, we are always able to find an optimal solution. This is no longer the case for the largest instances. However, even here, when we find a solution, it is always optimal.

The solutions of the problems with only the FRD (5.7) and the ones with FRD

Fleet size	Average cost	Average GAP	Average Time	Optimals	Found solution
10	560.88	0.03%	9.74	5	5
20	1036.18	0.00%	34.74	5	5
30	1495.46	0.00%	82.52	5	5
40	2003.44	0.00%	117.13	5	5
50	2476.67	0.00%	194.27	5	5
60	2956.18	0.00%	272.88	5	5
70	3416.63	0.00%	383.25	5	5
80	3891.43	0.00%	384.74	5	5
90	4370.27	0.00%	335.57	5	5
100	4839.64	0.00%	724.46	5	5

Table 5.4: Summary of the results obtained optimizing energy and FRD. For the detailed results check Table 5.8

	Energy	FRD	Deg	Total	GAP	Time
10_1	261.76	163.78	192.52	618.07	4.14%	7200
10_2	283.99	190.40	207.06	681.45	2.46%	7200
10_3	290.04	203.82	220.77	714.63	4.14%	7200
10_4	276.41	195.31	216.25	687.97	8.06%	7200
10_5	257.75	199.21	185.88	642.84	3.32%	7200
20_1	475.90	285.43	413.18	1174.51	5.98%	7200
20_2	486.73	319.31	425.44	1231.47	5.26%	7200
20_3	503.55	305.74	431.18	1240.47	3.45%	7200
20_4	465.89	317.95	396.87	1180.70	3.91%	7200
20_5	465.15	276.11	395.05	1136.31	4.92%	7200
30_1	667.14	455.48	613.17	1735.79	4.97%	7200
30_2						7200
30_3	692.07	407.52	625.75	1725.34	3.69%	7200
30_4	675.51	506.24	613.60	1795.36	4.56%	7200
30_5	643.75	385.98	581.53	1611.26	3.88%	7200
40_1						7200
40_2						7200
40_3	894.13	571.74	829.06	2294.93	3.70%	7200
40_4	874.96	590.03	813.43	2278.42	4.35%	7200
40_5						7200

Table 5.5: Optimization of degradation costs

and energy (5.8) are summarized in Table 5.3 and in Table 5.4. In both situations, the solver is always able to find an optimal solution. Furthermore, the solver is rally fast in finding solutions as it takes less 15 minutes even for the largest instances.

We have very good results in both cases, but the average time is lower in the instances with only FRD costs. However, for the first step of our heuristic we have decided to optimize both energy and FRD costs. Indeed, as it is shown in Table 5.4, we are able to achieve optimal solutions in less than 15 minutes while optimizing already two different costs.

We reported now in Table 5.9 the results obtained with our heuristic. For every instance we report the results of the two steps. Therefore, the values under the column "First step" refer to the results of the problem where we optimize energy and FRD costs. The results under the column "Second step" refer to the model of the second step, that is the EEV-CSP-V2Gindeed.

It is interesting to notice that with the second step we are able to improve the degradation costs of the first step of 2.08%. This quantity is computed as the ratio of the difference of the two costs and the degradation costs in the first step. We computed the same quantity for the total costs in the two steps and there is a global improvement of 0.87%. We have already remarked that the first step is really

	Energy	FRD	Deg	Total	GAP	Time
10_1	245.93	260.41	277.24	783.59	0.01%	17
10_2	265.03	266.09	326.44	857.57	0.09%	10
10_3	273.86	265.60	312.04	851.51	0.10%	6
10_4	262.66	267.88	340.84	871.38	0.01%	21
10_5	243.71	250.89	283.31	777.90	0.09%	20
20_1	442.89	509.61	623.31	1575.80	0.02%	41
20_2	454.74	530.77	488.93	1474.45	0.07%	131
20_3	469.13	543.13	536.44	1548.71	0.06%	36
20_4	434.23	492.06	483.24	1409.53	0.05%	57
20_5	429.74	483.39	522.82	1435.96	0.05%	44
30_1	627.99	741.41	677.60	2047.00	0.08%	116
30_2	633.49	749.72	780.04	2163.26	0.10%	343
30_3	645.63	766.10	814.51	2226.23	0.08%	70
30_4	629.10	740.32	715.65	2085.07	0.03%	290
30_5	604.33	685.57	675.78	1965.67	0.09%	107
40_1	849.66	1037.82	1075.32	2962.80	0.08%	320
40_2	832.21	996.16	970.35	2798.72	0.08%	272
40_3	831.68	1000.72	949.79	2782.18	0.05%	315
40_4	811.79	961.18	1050.04	2823.02	0.05%	328
40_5	813.76	967.74	956.44	2737.94	0.04%	366
50_1	1032.76	1247.10	1224.51	3504.37	0.05%	1555
50_2	1019.41	1219.04	1183.82	3422.28	0.09%	2505
50_3	1014.04	1220.49	1119.71	3354.23	0.07%	468
50_4	1012.55	1199.37	1124.58	3336.50	0.10%	381
50_5	999.54	1191.02	1131.66	3322.22	0.04%	193
60_1	1229.87	1496.62	1381.70	4108.19	0.04%	3836
60_2	1214.62	1458.81	1436.51	4109.94	0.03%	6853
60_3	1191.49	1426.78	1434.71	4052.99	0.09%	788
60_4	1192.70	1423.84	1374.89	3991.43	0.03%	707
60_5	1188.51	1420.71	1471.24	4080.46	0.06%	546
70_1	1428.73	1750.94	1784.03	4963.69	0.10%	625
70_2						7202
70_3	1355.57	1618.34	1516.22	4490.13	0.08%	614
70_4	1378.00	1662.04	1518.11	4558.15	0.05%	5812
70_5	1391.14	1679.41	1563.24	4633.80	0.02%	3043
80_1						7201
80_2						7202
80_3	1554.51	1877.17	1879.64	5311.32	0.09%	726
80_4	1567.30	1893.62	1898.11	5359.02	0.07%	932
80_5	1570.52	1894.83	1628.11	5093.45	0.10%	6771
90_1						7202
90_2	1761.42	2109.75	2135.91	6007.08	0.01%	4641
90_3						7202
90_4	1762.18	2150.46	2141.64	6054.28	0.09%	851
90_5	1770.29	2152.21	1998.11	5920.61	0.03%	6955
100_1						7202
100_2	1942.91	2319.89	2214.05	6476.85	0.01%	5270
100_3	1933.43	2330.42	2295.10	6558.95	0.10%	5860
100_4	1944.40	2356.67	2104.11	6405.18	0.05%	4819
100_5	1945.81	2344.44	2441.50	6731.75	0.03%	4443

Table 5.6: Optimization of energy costs

	Energy	FRD	Deg	Total	GAP	Time
10_1	263.73	75.62	192.65	532.00	0.05%	11
10_2	283.42	79.76	208.63	571.81	0.00%	8
10_3	292.76	80.85	221.46	595.07	0.00%	11
10_4	281.83	77.72	221.18	580.74	0.03%	11
10_5	261.90	71.98	191.38	525.26	0.00%	11
20_1	478.86	139.05	418.31	1036.22	0.00%	40
20_2	492.10	139.59	426.24	1057.93	0.00%	43
20_3	506.55	143.86	435.72	1086.13	0.00%	27
20_4	469.99	133.17	401.03	1004.19	0.00%	44
20_5	466.19	130.68	398.27	995.13	0.00%	38
30_1	681.19	198.72	613.25	1493.17	0.00%	72
30_2	688.50	194.56	630.51	1513.57	0.00%	93
30_3	700.69	201.17	635.55	1537.41	0.00%	56
30_4	683.85	193.23	621.68	1498.76	0.00%	104
30_5	657.09	185.54	585.08	1427.71	0.00%	57
40_1	923.80	265.37	886.08	2075.25	0.00%	170
40_2	906.71	257.27	847.15	2011.12	0.00%	137
40_3	904.06	264.04	851.27	2019.37	0.00%	162
40_4	884.32	250.83	819.45	1954.60	0.00%	132
40_5	886.50	251.46	830.88	1968.84	0.00%	119
50_1	1124.75	326.06	1074.67	2525.48	0.00%	156
50_2	1111.82	316.21	1058.80	2486.82	0.00%	146
50_3	1104.35	316.36	1035.11	2455.82	0.08%	161
50_4	1104.17	314.01	1039.35	2457.52	0.00%	191
50_5	1090.24	310.01	1038.08	2438.33	0.00%	214
60_1	1340.17	388.28	1302.99	3031.44	0.00%	240
60_2	1326.48	377.89	1294.88	2999.26	0.00%	612
60_3	1297.92	373.07	1225.35	2896.35	0.00%	125
60_4	1302.27	371.79	1244.61	2918.67	0.00%	218
60_5	1297.53	369.57	1257.36	2924.46	0.00%	287
70_1	1557.30	450.61	1519.83	3527.75	0.00%	325
70_2	1510.96	431.62	1467.90	3410.48	0.00%	451
70_3	1480.14	422.52	1410.69	3313.36	0.00%	228
70_4	1504.05	431.35	1451.04	3386.43	0.00%	289
70_5	1519.03	433.22	1476.46	3428.70	0.00%	272
80_1	1762.26	507.58	1724.09	3993.93	0.00%	321
80_2	1727.14	493.02	1682.49	3902.64	0.00%	347
80_3	1697.28	484.85	1630.22	3812.36	0.00%	432
80_4	1711.09	490.70	1656.43	3858.22	0.00%	290
80_5	1715.39	489.65	1674.26	3879.30	0.00%	365
90_1	1961.68	564.67	1936.44	4462.79	0.00%	380
90_2	1926.96	550.89	1898.08	4375.93	0.00%	493
90_3	1907.78	546.99	1848.08	4302.85	0.00%	284
90_4	1923.96	550.00	1863.53	4337.49	0.00%	403
90_5	1934.15	552.51	1897.56	4384.22	0.00%	438
100_1	2161.54	623.68	2129.65	4914.86	0.00%	407
100_2	2126.55	609.81	2104.73	4841.09	0.00%	539
100_3	2112.49	603.76	2050.31	4766.56	0.00%	431
100_4	2124.92	609.32	2082.07	4816.31	0.00%	531
100_5	2127.79	608.15	2082.72	4818.66	0.00%	541

Table 5.7: Optimization of FRD costs

	Energy	FRD	Deg	Total	GAP	Time
10_1	263.72	197.18	75.58	536.48	0.00%	11.81
10_2	283.37	208.78	79.95	572.10	0.04%	7.48
10_3	292.72	222.16	81.03	595.91	0.04%	7.03
10_4	281.75	219.20	78.10	579.04	0.09%	11.95
10_5	261.90	186.99	71.98	520.87	0.00%	10.43
20_1	478.86	415.74	139.05	1033.65	0.00%	28.43
20_2	492.09	429.88	139.70	1061.67	0.02%	32.96
20_3	506.55	438.52	143.86	1088.93	0.00%	30.56
20_4	469.99	398.77	133.17	1001.94	0.00%	39.75
20_5	466.19	397.84	130.68	994.71	0.00%	41.99
30_1	681.19	619.09	198.72	1499.00	0.00%	87.22
30_2	688.50	627.83	194.56	1510.89	0.00%	90.26
30_3	700.69	633.03	201.17	1534.89	0.00%	41.70
30_4	683.85	621.41	193.23	1498.49	0.00%	102.69
30_5	657.09	591.39	185.54	1434.02	0.00%	90.71
40_1	923.80	867.58	265.37	2056.76	0.00%	93.53
40_2	906.71	854.88	257.27	2018.86	0.00%	91.85
40_3	904.06	841.75	264.04	2009.85	0.00%	123.24
40_4	884.32	820.82	250.83	1955.97	0.00%	151.28
40_5	886.50	837.80	251.46	1975.76	0.00%	125.74
50_1	1124.75	1074.69	326.06	2525.50	0.00%	176.24
50_2	1111.82	1061.70	316.21	2489.73	0.00%	239.04
50_3	1104.29	1039.30	316.13	2459.71	0.00%	131.05
50_4	1104.17	1045.31	314.01	2463.49	0.00%	232.61
50_5	1090.24	1044.68	310.01	2444.92	0.00%	192.41
60_1	1340.17	1315.10	388.28	3043.54	0.00%	322.69
60_2	1326.48	1290.09	377.89	2994.46	0.00%	221.86
60_3	1297.92	1235.75	373.07	2906.75	0.00%	238.58
60_4	1302.27	1242.62	371.79	2916.68	0.00%	306.51
60_5	1297.53	1252.39	369.57	2919.49	0.00%	274.78
70_1	1557.30	1511.17	450.61	3519.08	0.00%	254.18
70_2	1510.96	1485.97	431.62	3428.55	0.00%	704.83
70_3	1480.14	1430.35	422.52	3333.02	0.00%	298.81
70_4	1504.05	1441.32	431.35	3376.72	0.00%	337.05
70_5	1519.03	1473.55	433.22	3425.80	0.00%	321.36
80_1	1762.26	1723.77	507.58	3993.61	0.00%	460.29
80_2	1727.14	1685.72	493.02	3905.87	0.00%	387.37
80_3	1697.28	1629.63	484.85	3811.77	0.00%	303.38
80_4	1711.09	1668.25	490.70	3870.05	0.00%	335.02
80_5	1715.39	1670.79	489.65	3875.83	0.00%	437.62
90_1	1961.68	1942.09	564.67	4468.44	0.00%	339.63
90_2	1926.96	1892.42	550.89	4370.27	0.00%	411.66
90_3	1907.78	1844.07	546.99	4298.84	0.00%	267.63
90_4	1923.96	1868.65	550.00	4342.61	0.00%	346.56
90_5	1934.15	1884.53	552.51	4371.19	0.00%	312.36
100_1	2161.54	2169.43	623.68	4954.65	0.00%	1579.46
100_2	2126.55	2103.88	609.81	4840.24	0.00%	421.33
100_3	2112.49	2054.33	603.76	4770.58	0.00%	786.84
100_4	2124.92	2074.34	609.32	4808.58	0.00%	393.04
100_5	2127.79	2088.21	608.15	4824.15	0.00%	441.62

Table 5.8: Optimization of energy and FRD costs

	First step						Second step					
	Energy	FRD	Deg	Total	Time	GAP	Energy	FRD	Deg	Total	Time	GAP
10_1	263.7	75.6	199.8	539.1	11	0.00%	263.7	75.6	192.5	531.8	7200	1.86%
10_2	283.4	80.0	210.8	574.1	7	0.04%	283.4	79.8	208.5	571.6	7200	1.13%
10_3	292.7	81.0	224.8	598.6	7	0.04%	292.8	80.8	220.8	594.4	7200	1.47%
10_4	281.7	78.1	222.2	582.0	12	0.09%	281.6	78.6	219.2	579.5	7200	2.82%
10_5	261.9	72.0	189.0	522.8	10	0.00%	261.9	72.0	187.5	521.4	7200	1.49%
20_1	478.9	139.0	420.9	1038.8	27	0.00%	478.9	139.0	413.2	1031.1	7200	2.32%
20_2	492.1	139.7	434.8	1066.6	34	0.02%	492.1	139.6	425.4	1057.1	7200	2.24%
20_3	506.6	143.9	443.1	1093.6	30	0.00%	506.6	143.9	432.6	1083.0	7200	1.54%
20_4	470.0	133.2	403.3	1006.4	38	0.00%	470.0	133.2	396.9	1000.0	7200	1.58%
20_5	466.2	130.7	402.7	999.6	41	0.00%	466.2	130.7	395.1	991.9	7200	1.96%
30_1	681.2	198.7	626.6	1506.5	83	0.00%	681.2	198.7	613.2	1493.1	7200	2.05%
30_2	688.5	194.6	634.7	1517.8	84	0.00%	688.5	194.6	625.6	1508.6	7200	2.39%
30_3	700.7	201.2	639.7	1541.6	44	0.00%	700.7	201.2	625.8	1527.6	7200	1.51%
30_4	683.9	193.2	628.9	1506.0	95	0.00%	683.9	193.2	613.6	1490.7	7200	1.85%
30_5	657.1	185.5	598.4	1441.0	87	0.00%	657.1	185.5	581.5	1424.2	7200	1.63%
40_1	923.8	265.4	878.1	2067.3	91	0.00%	923.8	265.4	861.0	2050.2	7200	2.14%
40_2	906.7	257.3	864.4	2028.3	97	0.00%	906.7	257.3	845.9	2009.8	7200	2.35%
40_3	904.1	264.0	850.0	2018.1	116	0.00%	904.1	264.0	829.1	1997.2	7200	1.56%
40_4	884.3	250.8	829.5	1964.6	141	0.00%	884.3	250.8	813.4	1948.6	7200	1.85%
40_5	886.5	251.5	847.1	1985.1	127	0.00%	886.5	251.5	823.4	1961.4	7200	2.24%
50_1	1124.7	326.1	1087.8	2538.6	180	0.00%	1124.7	326.1	1069.7	2520.6	7200	2.38%
50_2	1111.8	316.2	1074.7	2502.7	232	0.00%	1111.8	316.2	1056.1	2484.1	7200	2.51%
50_3	1104.3	316.1	1050.1	2470.5	133	0.00%	1104.3	316.1	1024.8	2445.2	7200	1.49%
50_4	1104.2	314.0	1056.8	2475.0	235	0.00%	1104.2	314.0	1033.8	2452.0	7200	1.93%
50_5	1090.2	310.0	1057.9	2458.1	202	0.00%	1090.2	310.0	1025.6	2425.8	7200	2.16%
60_1	1340.2	388.3	1332.2	3060.7	331	0.00%	1340.2	388.3	1292.5	3020.9	7200	2.58%
60_2	1326.5	377.9	1306.1	3010.5	210	0.00%	1326.5	377.9	1277.7	2982.1	7200	2.56%
60_3	1297.9	373.1	1248.2	2919.2	231	0.00%	1297.9	373.1	1220.2	2891.2	7200	1.58%
60_4	1302.3	371.8	1255.7	2929.7	310	0.00%	1302.3	371.8	1236.5	2910.6	7200	2.01%
60_5	1297.5	369.6	1266.7	2933.8	261	0.00%	1297.5	369.6	1235.1	2902.2	7200	2.18%
70_1	1557.3	450.6	1528.9	3536.8	247	0.00%	1557.3	450.6	1505.6	3513.5	7200	2.31%
70_2	1511.0	431.6	1504.5	3447.1	675	0.00%	1511.0	431.6	1459.6	3402.2	7200	2.45%
70_3	1480.1	422.5	1445.3	3347.9	282	0.00%	1480.1	422.5	1401.3	3304.0	7200	1.61%
70_4	1504.0	431.4	1457.3	3392.7	329	0.00%	1504.0	431.4	1433.4	3368.8	7200	1.85%
70_5	1519.0	433.2	1492.4	3444.6	332	0.00%	1519.0	433.2	1461.7	3414.0	7200	2.28%
80_1	1762.3	507.6	1742.9	4012.8	454	0.00%	1762.3	507.6	1705.9	3975.7	7200	2.18%
80_2	1727.1	493.0	1704.9	3925.0	375	0.00%	1727.1	493.0	1675.8	3895.9	7200	2.38%
80_3	1697.3	484.9	1646.8	3829.0	282	0.00%	1697.3	484.9	1620.0	3802.1	7200	1.68%
80_4	1711.1	490.7	1687.8	3889.6	328	0.00%	1711.1	490.7	1648.9	3850.7	7200	2.06%
80_5	1715.4	489.6	1691.2	3896.2	422	0.00%	1715.4	489.6	1661.3	3866.4	7200	2.31%
90_1	1961.7	564.7	1966.6	4492.9	349	0.00%	1961.7	564.7	1921.0	4447.4	7200	2.48%
90_2	1927.0	550.9	1915.0	4392.8	394	0.00%	1927.0	550.9	1880.5	4358.3	7200	2.36%
90_3	1907.8	547.0	1863.6	4318.4	262	0.00%	1907.8	547.0	1832.6	4287.4	7200	1.73%
90_4	1924.0	550.0	1888.3	4362.3	335	0.00%	1924.0	550.0	1857.3	4331.2	7200	1.92%
90_5	1934.2	552.5	1906.7	4393.4	285	0.00%	1934.2	552.5	1880.1	4366.8	7200	2.20%
100_1	2161.5	623.7	2198.4	4983.7	1489	0.00%	2161.5	623.7	2118.7	4904.0	7200	2.38%
100_2	2126.6	609.8	2129.5	4865.9	409	0.00%	2126.6	609.8	2080.6	4816.9	7200	2.35%
100_3	2112.5	603.8	2078.2	4794.5	751	0.00%	2112.5	603.8	2038.2	4754.4	7200	1.77%
100_4	2124.9	609.3	2097.0	4831.3	382	0.00%	2124.9	609.3	2068.0	4802.2	7200	2.10%
100_5	2127.8	608.2	2112.8	4848.7	418	0.00%	2127.8	608.2	2074.5	4810.4	7200	2.24%

Table 5.9: Heuristic results

fast and solve up to optimality. On the other hand the second step solution is not optimal and the time limit is always reached. Nevertheless, thanks to this heuristic, it is possible to find solutions for all the instances, which is a great improvement if compared with the results of Table 5.1.

5.2   Managerial insights

In this section, we perform sensitivity analyses by varying a number of parameters from the base scenario. some perturbations of the parameters of the base case scenario of chapter 4 are done. Then, the problems are solved with the heuristic in section 3.8.

The aim of these experiments is twofold. First of all, changing some parameters could affect the solution procedure. But most importantly, we aim at investigating whether V2G technologies can be beneficial for the operation of the fleet. Indeed in all the solutions of the base case scenario (5.9), the total amount of energy discharged is null. This means that for this particular problem, it is not convenient to use V2G technologies. Namely, a fleet of EVs instead of EV-V2Gs would lead to the same results. The reasons behind these are not straightforward. The first hypothesis could be that this is due to the degradation costs. Indeed, in order to be able to discharge EBs, they need to be overcharged and we know that overcharging usually increases damages of batteries. Another reason could be due to a lack of flexibility in the base case scenario. Indeed, apart from night time, EBs do not spend a lot of time in the depot. The time they spend in the depot therefore, could not be enough both for charging and discharging. Or maybe the number of chargers in the depot are not enough to allow it. Finally, since the the plan is over 24 hours and the cost incurred for the FRD component is high when compared to other costs, the maximum power itself could discourage the use of V2Gs, contradicting the idea of the peak-shaving effect of V2Gs. Indeed, even if V2Gs can for sure decrease the power retrieved from the grid while discharging, the higher level of SOC they require in order to do that could lead to a higher load in other periods. Thus, V2Gs might not be convenient. Therefore, it would also be interesting to see if restricting the grid capacity without modifying the degradation costs, V2Gs are employed to find a feasible solution.

Following these ideas, the tests performed are aimed at perturbing the degradation costs (5.2.1), increasing the number of chargers in the depot (5.2.2), adding other vehicles which have more flexibility in the route planning (5.2.3), modifying the costs for the maximum power (5.2.4) and decreasing the capacity of the grid (5.2.5).

5.2.1   Impact of degradation costs

As already explained, it is worth investigating the part of the EEV-CPS-V2G related to the battery degradation. Indeed, in order to be able to discharge, EBs must be charged longer as they need to store more energy than what they would have needed otherwise. Since the wear cost function increases with the state of charge, this would lead to a higher contribution of the degradation part. If the

increase of degradation costs is higher than the benefits due to the usage of V2G technologies, then V2G would not be exploited.

At first, the wear cost function is modified using only 2 points to calibrate it. Namely, we set $|\mathcal{D}| = 2$, $L = 0.5$ and w_d of $0.100, 0.136$. Then the degradation costs are modified basing on battery price of 2030 (*New Energy Outlook 2020*). The results for this setting are reported in Table 5.10.

In addition to the values reported before, here we add the columns "V2G" that says whether V2G technologies are used or not and their percentage usage (V2G%). The V2G percentage usage is computed as the quantity of energy discharged by the fleet and the total quantity of energy of the planning period. The total cost, GAP optimality and time occurred in the base case are also reported.

We have also run the instances with a different configuration of the wear costs parameters w_d. In particular, we have considered batteries at half price. Starting from the initial price of 51 € and with 4 interpolation points for the wear cost function, we have obtained $0.060, 0.064, 0.072, 0.098$ as parameters for the wear cost function. The results for this setting are reported in Table 5.11.

Unfortunately, V2G are not beneficial under these conditions, not even when considering half contribution for the degradation costs. It is also interesting to notice that, even if the variables soc_{pdk}^{+} (used for degradation costs) seem as one of the possible causes that make the problem hard to be solved, when they are halved the problem does not become easier. Indeed the GAP in this scenario is always higher than the base scenario.

5.2.2 Impact of the number of chargers

Another aspect that could be beneficial both for the solution quality and the usage of V2G is the number of available chargers. As already discussed (chapter 2), many other approaches do not impose restrictions on the number of chargers. In this spirit we assume that every EB is equipped with both a slow and a fast charger. Namely, this means that the coupling constraints (3.115) are removed from the EEV-CPS-V2G formulation. The results for this setting are reported in Table 5.12.

Also in this situation V2G vehicles are not used. Adding this type of flexibility to the setting is not beneficial. Notice however that, as expected, for most of the instances in the perturbed scenario, the optimality GAP is better than the one in the base case.

5.2.3 Impact of fleet scheduling

In this section we add a number of EBs without routes assigned. Also this case is inspired from the real applications. Indeed, depots typically maintain a few buses on standby in case of emergency. The idea is that being in the depot, they could be able to charge in every moment, and discharge when most needed. For every

	2 breakpoints wear cost function							Base case		
	Energy	FRD	Deg	Total	GAP	Time	V2G	V2G %	Total	GAP	Time
10_1	263.72	75.58	195.16	534.46	2.19%	7200	0	0	531.82	1.86%	7211
10_2	283.42	79.76	214.02	577.20	1.79%	7200	0	0	571.62	1.13%	7207
10_3	292.76	80.85	224.30	597.90	1.78%	7200	0	0	594.38	1.47%	7207
10_4	280.35	84.48	219.71	584.53	3.24%	7200	0	0	579.46	2.82%	7211
10_5	261.21	75.09	190.34	526.64	2.38%	7200	0	0	521.37	1.49%	7210
20_1	478.86	139.05	418.91	1036.82	2.77%	7200	0	0	1031.09	2.32%	7228
20_2	492.10	139.59	432.38	1064.07	2.60%	7200	0	0	1057.13	2.24%	7233
20_3	506.55	143.86	441.64	1092.05	2.24%	7200	0	0	1083.04	1.54%	7230
20_4	469.99	133.17	403.62	1006.78	2.14%	7200	0	0	1000.03	1.58%	7239
20_5	466.19	130.68	402.21	999.07	2.68%	7200	0	0	991.91	1.96%	7241
30_1	681.19	198.72	622.53	1502.45	2.66%	7200	0	0	1493.09	2.05%	7284
30_2	688.50	194.56	634.92	1517.98	2.91%	7200	0	0	1508.64	2.39%	7283
30_3	700.69	201.17	637.66	1539.52	2.22%	7200	0	0	1527.61	1.51%	7242
30_4	683.85	193.23	624.27	1501.35	2.51%	7200	0	0	1490.68	1.85%	7297
30_5	657.09	185.54	593.99	1436.62	2.46%	7200	0	0	1424.15	1.63%	7289
40_1	923.80	265.37	876.62	2065.79	2.76%	7200	0	0	2050.17	2.14%	7288
40_2	906.71	257.27	859.11	2023.09	2.89%	7200	0	0	2009.84	2.35%	7290
40_3	904.06	264.04	844.33	2012.43	2.19%	7200	0	0	1997.16	1.56%	7314
40_4	884.32	250.83	826.80	1961.95	2.44%	7200	0	0	1948.58	1.85%	7345
40_5	886.50	251.46	837.41	1975.37	2.87%	7200	0	0	1961.39	2.24%	7318
50_1	1124.75	326.06	1089.27	2540.08	3.05%	7200	0	0	2520.55	2.38%	7374
50_2	1111.82	316.21	1073.32	2501.35	3.07%	7200	0	0	2484.09	2.51%	7421
50_3	1104.29	316.13	1043.49	2463.90	2.11%	7200	0	0	2445.18	1.49%	7334
50_4	1104.17	314.01	1052.45	2470.63	2.57%	7200	0	0	2451.98	1.93%	7413
50_5	1090.24	310.01	1044.85	2445.10	2.85%	7200	0	0	2425.84	2.16%	7393
60_1	1340.17	388.28	1315.77	3044.22	3.23%	7200	0	0	3020.90	2.58%	7527
60_2	1326.46	377.99	1299.87	3004.32	3.16%	7200	0	0	2982.09	2.56%	7405
60_3	1297.92	373.07	1241.59	2912.59	2.13%	7200	0	0	2891.20	1.58%	7429
60_4	1302.27	371.79	1256.07	2930.13	2.58%	7200	0	0	2910.59	2.01%	7496
60_5	1297.53	369.57	1256.08	2923.18	2.83%	7200	0	0	2902.18	2.18%	7439
70_1	1557.30	450.61	1531.61	3539.53	2.94%	7200	0	0	3513.50	2.31%	7447
70_2	1510.96	431.62	1481.08	3423.65	2.98%	7200	0	0	3402.22	2.45%	7878
70_3	1480.14	422.52	1424.57	3327.24	2.23%	7200	0	0	3303.96	1.61%	7519
70_4	1504.05	431.35	1458.79	3394.18	2.54%	7200	0	0	3368.81	1.85%	7524
70_5	1519.03	433.22	1489.48	3441.73	2.90%	7200	0	0	3413.96	2.28%	7519
80_1	1762.26	507.58	1736.47	4006.31	2.85%	7200	0	0	3975.69	2.18%	7649
80_2	1727.14	493.02	1704.38	3924.53	2.99%	7200	0	0	3895.93	2.38%	7563
80_3	1697.28	484.85	1649.51	3831.64	2.34%	7200	0	0	3802.14	1.68%	7462
80_4	1711.09	490.70	1677.44	3879.23	2.70%	7200	0	0	3850.70	2.06%	7509
80_5	1715.39	489.65	1691.11	3896.15	3.00%	7200	0	0	3866.38	2.31%	7614
90_1	1961.64	564.84	1952.91	4479.39	3.14%	7200	0	0	4447.36	2.48%	7549
90_2	1926.96	550.89	1913.22	4391.07	2.99%	7200	0	0	4358.33	2.36%	7602
90_3	1907.78	546.99	1866.27	4321.05	2.43%	7200	0	0	4287.41	1.73%	7465
90_4	1923.96	550.00	1890.74	4364.71	2.56%	7200	0	0	4331.24	1.92%	7539
90_5	1934.15	552.51	1913.43	4400.09	2.85%	7200	0	0	4366.76	2.20%	7477
100_1	2161.54	623.68	2152.90	4938.11	3.04%	7200	0	0	4903.96	2.38%	8623
100_2	2126.55	609.81	2115.87	4852.23	2.98%	7200	0	0	4816.93	2.35%	7608
100_3	2112.49	603.76	2075.30	4791.55	2.47%	7200	0	0	4754.42	1.77%	7963
100_4	2124.92	609.32	2104.32	4838.56	2.76%	7200	0	0	4802.23	2.10%	7609
100_5	2127.79	608.15	2107.95	4843.89	2.86%	7200	0	0	4810.44	2.24%	7200

Table 5.10: Results obtained with the wear cost function calibrated over two points

	Half battery price								Base case		
	Energy	FRD	Deg	Total	GAP	Time	V2G	V2G %	Total	GAP	Time
10_1	263.72	75.58	119.00	458.29	2.08%	7212	0	0	531.82	1.86%	7200
10_2	283.42	79.76	128.83	492.00	1.29%	7207	0	0	571.62	1.13%	7200
10_3	292.76	80.85	136.36	509.96	1.54%	7207	0	0	594.38	1.47%	7200
10_4	281.69	78.38	134.92	494.98	2.40%	7212	0	0	579.46	2.82%	7200
10_5	261.90	71.98	115.35	449.22	1.50%	7210	0	0	521.37	1.49%	7200
20_1	478.86	139.05	255.17	873.08	2.31%	7229	0	0	1031.09	2.32%	7200
20_2	492.10	139.59	262.20	893.89	2.15%	7233	0	0	1057.13	2.24%	7200
20_3	506.55	143.86	267.36	917.76	1.63%	7231	0	0	1083.04	1.54%	7200
20_4	469.99	133.17	244.79	847.96	1.81%	7240	0	0	1000.03	1.58%	7200
20_5	466.19	130.68	243.76	840.63	2.09%	7243	0	0	991.91	1.96%	7200
30_1	681.19	198.72	378.50	1258.42	2.17%	7292	0	0	1493.09	2.05%	7200
30_2	688.50	194.56	386.00	1269.06	2.35%	7285	0	0	1508.64	2.39%	7200
30_3	700.69	201.17	385.92	1287.78	1.72%	7242	0	0	1527.61	1.51%	7200
30_4	683.85	193.23	377.87	1254.95	2.00%	7303	0	0	1490.68	1.85%	7200
30_5	657.09	185.54	357.95	1200.58	1.82%	7291	0	0	1424.15	1.63%	7200
40_1	923.80	265.37	531.21	1720.38	2.19%	7289	0	0	2050.17	2.14%	7200
40_2	906.71	257.27	522.04	1686.02	2.38%	7289	0	0	2009.84	2.35%	7200
40_3	904.06	264.04	511.86	1679.96	1.83%	7318	0	0	1997.16	1.56%	7200
40_4	884.32	250.83	501.17	1636.31	2.00%	7354	0	0	1948.58	1.85%	7200
40_5	886.50	251.46	508.78	1646.74	2.34%	7319	0	0	1961.39	2.24%	7200
50_1	1124.75	326.06	660.49	2111.30	2.44%	7390	0	0	2520.55	2.38%	7200
50_2	1111.82	316.21	654.09	2082.11	2.61%	7435	0	0	2484.09	2.51%	7200
50_3	1104.29	316.13	635.35	2055.76	1.89%	7335	0	0	2445.18	1.49%	7200
50_4	1104.17	314.01	637.20	2055.38	2.04%	7418	0	0	2451.98	1.93%	7200
50_5	1090.24	310.01	636.66	2036.91	2.49%	7401	0	0	2425.84	2.16%	7200
60_1	1340.17	388.28	797.58	2526.03	2.54%	7527	0	0	3020.90	2.58%	7200
60_2	1326.48	377.89	790.29	2494.66	2.65%	7411	0	0	2982.09	2.56%	7200
60_3	1297.92	373.07	752.54	2423.54	1.79%	7430	0	0	2891.20	1.58%	7200
60_4	1302.27	371.79	767.12	2441.17	2.34%	7504	0	0	2910.59	2.01%	7200
60_5	1297.53	369.57	762.42	2429.52	2.33%	7450	0	0	2902.18	2.18%	7200
70_1	1557.30	450.61	931.02	2938.94	2.44%	7461	0	0	3513.50	2.31%	7200
70_2	1510.96	431.62	902.79	2845.37	2.62%	7902	0	0	3402.22	2.45%	7200
70_3	1480.14	422.52	878.59	2781.26	2.42%	7490	0	0	3303.96	1.61%	7200
70_4	1504.05	431.35	888.73	2824.12	2.22%	7535	0	0	3368.81	1.85%	7200
70_5	1519.03	433.22	902.45	2854.70	2.39%	7546	0	0	3413.96	2.28%	7200
80_1	1762.26	507.58	1057.16	3327.00	2.41%	7670	0	0	3975.69	2.18%	7200
80_2	1727.14	493.02	1039.15	3259.31	2.61%	7576	0	0	3895.93	2.38%	7200
80_3	1697.28	484.85	1004.16	3186.29	2.09%	7497	0	0	3802.14	1.68%	7200
80_4	1711.05	490.89	1023.20	3225.14	2.39%	7537	0	0	3850.70	2.06%	7200
80_5	1715.39	489.65	1028.26	3233.30	2.52%	7632	0	0	3866.38	2.31%	7200
90_1	1961.68	564.67	1197.30	3723.65	2.83%	7570	0	0	4447.36	2.48%	7200
90_2	1926.96	550.89	1164.14	3641.99	2.59%	7599	0	0	4358.33	2.36%	7200
90_3	1907.78	546.99	1135.13	3589.91	2.14%	7454	0	0	4287.41	1.73%	7200
90_4	1923.89	550.41	1151.54	3625.83	2.30%	7553	0	0	4331.24	1.92%	7200
90_5	1934.15	552.51	1163.78	3650.44	2.45%	7497	0	0	4366.76	2.20%	7200
100_1	2161.54	623.68	1323.32	4108.53	2.86%	8724	0	0	4903.96	2.38%	7200
100_2	2126.55	609.81	1295.39	4031.75	2.78%	7608	0	0	4816.93	2.35%	7200
100_3	2112.49	603.76	1265.37	3981.62	2.26%	7921	0	0	4754.42	1.77%	7200
100_4	2124.84	609.66	1283.60	4018.11	2.47%	7583	0	0	4802.23	2.10%	7200
100_5	2127.79	608.15	1286.39	4022.33	2.50%	7609	0	0	4810.44	2.24%	7200

Table 5.11: Results obtained with the initial price of battery is halved

	No charger restrictions								Base case		
	Energy	FRD	Deg	Total	GAP	Time	V2G	V2G %	Total	GAP	Time
10_1	263.72	75.58	192.52	531.82	1.67%	7200	0	0	531.82	1.86%	7212
10_2	283.42	79.76	208.45	571.62	1.13%	7200	0	0	571.62	1.13%	7209
10_3	292.76	80.85	220.77	594.38	1.42%	7200	0	0	594.38	1.47%	7209
10_4	281.64	78.59	219.24	579.46	2.77%	7200	0	0	579.46	2.82%	7215
10_5	261.90	71.98	187.49	521.37	1.49%	7200	0	0	521.37	1.49%	7212
20_1	478.86	139.05	413.18	1031.09	2.32%	7200	0	0	1031.09	2.32%	7235
20_2	492.10	139.59	425.44	1057.13	2.25%	7200	0	0	1057.13	2.24%	7238
20_3	506.55	143.86	432.63	1083.04	1.55%	7200	0	0	1083.04	1.54%	7230
20_4	469.99	133.17	396.87	1000.03	1.54%	7200	0	0	1000.03	1.58%	7232
20_5	466.19	130.68	395.05	991.91	1.98%	7200	0	0	991.91	1.96%	7244
30_1	681.19	198.72	613.17	1493.09	2.05%	7200	0	0	1493.09	2.05%	7300
30_2	688.50	194.56	625.58	1508.64	2.39%	7200	0	0	1508.64	2.39%	7288
30_3	700.69	201.17	625.75	1527.61	1.55%	7200	0	0	1527.61	1.51%	7254
30_4	683.85	193.23	613.60	1490.68	1.88%	7200	0	0	1490.68	1.85%	7273
30_5	657.09	185.54	581.53	1424.15	1.63%	7200	0	0	1424.15	1.63%	7307
40_1	923.80	265.37	860.99	2050.17	2.16%	7200	0	0	2050.17	2.14%	7306
40_2	906.71	257.27	845.87	2009.84	2.35%	7200	0	0	2009.84	2.35%	7327
40_3	904.06	264.04	829.06	1997.16	1.53%	7200	0	0	1997.16	1.56%	7285
40_4	884.32	250.83	813.43	1948.58	1.83%	7200	0	0	1948.58	1.85%	7341
40_5	886.50	251.46	823.43	1961.39	2.22%	7200	0	0	1961.39	2.24%	7333
50_1	1124.75	326.06	1069.81	2520.62	2.39%	7200	0	0	2520.55	2.38%	7379
50_2	1111.82	316.21	1056.07	2484.09	2.48%	7200	0	0	2484.09	2.51%	7348
50_3	1104.29	316.13	1024.76	2445.18	1.47%	7200	0	0	2445.18	1.49%	7338
50_4	1104.17	314.01	1033.80	2451.98	1.93%	7200	0	0	2451.98	1.93%	7338
50_5	1090.24	310.01	1025.59	2425.84	2.12%	7200	0	0	2425.84	2.16%	7356
60_1	1340.17	388.28	1292.45	3020.90	2.56%	7200	0	0	3020.90	2.58%	7449
60_2	1326.48	377.89	1278.27	2982.64	2.56%	7200	0	0	2982.09	2.56%	7452
60_3	1297.92	373.07	1220.21	2891.20	1.59%	7200	0	0	2891.20	1.58%	7378
60_4	1302.27	371.79	1236.53	2910.59	2.02%	7200	0	0	2910.59	2.01%	7456
60_5	1297.53	369.57	1235.07	2902.18	2.18%	7200	0	0	2902.18	2.18%	7401
70_1	1557.30	450.61	1505.59	3513.50	2.32%	7200	0	0	3513.50	2.31%	7464
70_2	1510.96	431.62	1459.64	3402.22	2.45%	7200	0	0	3402.22	2.45%	8275
70_3	1480.14	422.52	1401.29	3303.96	1.60%	7200	0	0	3303.96	1.61%	7408
70_4	1504.05	431.35	1433.41	3368.81	1.85%	7200	0	0	3368.81	1.85%	7426
70_5	1519.03	433.22	1461.72	3413.96	2.24%	7200	0	0	3413.96	2.28%	8303
80_1	1762.26	507.58	1705.85	3975.69	2.16%	7200	0	0	3975.69	2.18%	7551
80_2	1727.14	493.02	1674.99	3895.15	2.32%	7200	0	0	3895.93	2.38%	7648
80_3	1697.28	484.85	1620.01	3802.14	1.67%	7200	0	0	3802.14	1.68%	7628
80_4	1711.09	490.70	1648.91	3850.70	2.06%	7200	0	0	3850.70	2.06%	7644
80_5	1715.39	489.65	1661.34	3866.38	2.28%	7200	0	0	3866.38	2.31%	7457
90_1	1961.68	564.67	1921.27	4447.62	2.48%	7200	0	0	4447.36	2.48%	7669
90_2	1926.96	550.89	1882.81	4360.65	2.44%	7200	0	0	4358.33	2.36%	7521
90_3	1907.78	546.99	1832.63	4287.41	1.73%	7200	0	0	4287.41	1.73%	7544
90_4	1923.96	550.00	1855.39	4329.35	1.87%	7200	0	0	4331.24	1.92%	7609
90_5	1934.15	552.51	1879.93	4366.59	2.19%	7200	0	0	4366.76	2.20%	7905
100_1	2161.54	623.68	2117.90	4903.12	2.37%	7200	0	0	4903.96	2.38%	7636
100_2	2126.55	609.81	2080.29	4816.65	2.35%	7200	0	0	4816.93	2.35%	7854
100_3	2112.49	603.76	2038.17	4754.42	1.77%	7200	0	0	4754.42	1.77%	7685
100_4	2124.92	609.32	2068.70	4802.94	2.11%	7200	0	0	4802.23	2.10%	7663
100_5	2127.79	608.15	2072.01	4807.94	2.18%	7200	0	0	4810.44	2.24%	7619

Table 5.12: Results obtained with the assumption that every EB has a slow and a fast charger always at disposal

instance considered, a number of EBs equal to one third of the fleet is added. The results for this setting are reported in Table 5.13.

V2G technologies are employed in almost 30 instances out of 50. However, on average they are only account for the 0.46% of the total amount of energy that flows.

It is also interesting to notice that in some of these situations, V2Gs are not exploited because of the degradation costs. We remind that the solutions are obtained at first considering only energy and FRD costs, and as second step also the degradation. We have therefore two different solutions that can be compared. In Figure 5.1 we report the solutions for the first instance of 5.13:

As already explained, the panels we represent the scheduling of the fleet. Every line is associated with an EB. Blue lines are for the routes. The usage of a charger is represented by the green line, when they discharge by a red one. If the color is dark, it means that a fast charger is being used. In the first step (5.1a) the new EBs are using V2G technologies. They are charged and discharged during the period. When we consider also the degradation costs instead (5.1b), the new EBs are kept at the minimum level of SOC possible for the whole time. Basically in the second step, therefore in the solution of the EEV-CSP-V2G, they are completely ignored.

5.2.4 Impact of Facility related costs

In the base case study, we set the value of the FRD parameter F at $0.6 \,\text{\euro}/\text{kWh}$. We decrease the value of F by 50%, 25%, 1%, 0.5% and 0.25%. For sake of simplicity all the tables are not reported here but just a summary. In the first two cases, V2Gs are not exploited. Then there are very few instances when they are used. The most interesting part is that when the reduction of F is above 1%, the solver is not able to find a solution for the first step. This means that the FRD component of the solution drives the resolution. This also explains why the results of the model with energy and FRD costs (Table 5.8) are found faster than for the model with only energy (Table 5.6), despite the latter is a simpler case.

5.2.5 Impact of grid capacity

Lastly, the impact of the grid restriction is analyzed. The parameter G is decreased by the 10%, 30%, 50% and 70% from the value of the base case scenario. The idea behind this, is that V2G could be employed for necessity despite costs. Instances with 10% are not feasible. For the other cases V2Gs are not used. The results or this setting are reported in Table 5.14, Table 5.15 and Table 5.16.

5.2.6 Other cases

A last remark for the analysis of V2Gs usage, regards the base case scenario solved only optimizing energy costs. In all these instances indeed, V2G technologies

	Extra vehicles								Base case		
	Energy	FRD	Deg	Total	Time	GAP	V2G	V2G %	Total	Time	GAP
10_1	263.72	75.58	190.85	530.15	2.54%	7224	0	0.00%	531.817	1.86%	7200
10_2	283.42	79.76	206.62	569.79	1.91%	7227	0	0.00%	571.624	1.13%	7200
10_3	292.76	80.85	218.68	592.29	2.20%	7215	0	0.00%	594.382	1.47%	7200
10_4	281.64	78.59	215.98	576.21	3.41%	7226	0	0.00%	579.464	2.82%	7200
10_5	261.90	71.98	184.91	518.78	2.20%	7229	0	0.00%	521.369	1.49%	7200
20_1	478.86	139.05	409.21	1027.12	3.22%	7342	0	0.00%	1031.087	2.32%	7200
20_2	492.10	139.59	420.41	1052.10	3.01%	7292	0	0.00%	1057.130	2.24%	7200
20_3	506.55	143.86	428.76	1079.17	2.23%	7281	0	0.00%	1083.037	1.54%	7200
20_4	469.99	133.17	392.55	995.71	2.57%	7315	0	0.00%	1000.031	1.58%	7200
20_5	466.19	130.68	390.90	987.76	2.91%	7311	0	0.00%	991.913	1.96%	7200
30_1	681.19	198.72	607.09	1487.00	3.02%	7482	0	0.00%	1493.087	2.05%	7200
30_2	688.50	194.56	619.06	1502.12	3.27%	7460	0	0.00%	1508.636	2.39%	7200
30_3	700.69	201.17	619.06	1520.92	2.40%	7385	0	0.00%	1527.610	1.51%	7200
30_4	683.85	193.23	611.29	1488.37	3.17%	7447	0	0.00%	1490.685	1.85%	7200
30_5	657.09	185.54	573.89	1416.52	2.54%	7380	0	0.00%	1424.152	1.63%	7200
40_1	924.23	266.73	866.47	2057.42	3.82%	7507	1	0.44%	2050.168	2.14%	7200
40_2	907.03	258.98	854.63	2020.64	4.27%	7581	1	0.67%	2009.844	2.35%	7200
40_3	904.74	265.09	844.16	2013.99	3.79%	7556	1	0.74%	1997.159	1.56%	7200
40_4	884.32	250.83	811.59	1946.74	3.18%	7564	0	0.00%	1948.577	1.85%	7200
40_5	886.64	252.41	825.17	1964.21	3.77%	7495	1	0.23%	1961.389	2.24%	7200
50_1	1125.01	325.55	1068.52	2519.08	3.74%	7656	1	0.18%	2520.552	2.38%	7200
50_2	1114.51	313.74	1084.64	2512.89	4.97%	7979	1	1.52%	2484.094	2.51%	7200
50_3	1105.30	321.68	1051.90	2478.87	4.20%	7562	1	1.30%	2445.175	1.49%	7200
50_4	1104.48	313.52	1039.13	2457.13	3.50%	7576	1	0.18%	2451.979	1.93%	7200
50_5	1090.24	310.01	1015.24	2415.49	3.20%	8096	0	0.00%	2425.839	2.16%	7200
60_1	1339.96	389.85	1297.75	3027.55	4.15%	7896	0	0.00%	3020.901	2.58%	7200
60_2	1326.13	380.44	1276.38	2982.94	4.02%	7883	0	0.00%	2982.094	2.56%	7200
60_3	1298.17	379.99	1233.90	2912.06	3.69%	7814	1	0.66%	2891.205	1.58%	7200
60_4	1302.02	372.95	1250.79	2925.76	3.95%	7768	0	0.00%	2910.588	2.01%	7200
60_5	1297.53	369.57	1229.72	2896.83	3.47%	7741	0	0.00%	2902.176	2.18%	7200
70_1	1558.73	451.42	1535.41	3545.56	4.59%	7957	1	0.63%	3513.502	2.31%	7200
70_2	1512.38	431.72	1483.21	3427.31	4.65%	8004	1	0.81%	3402.218	2.45%	7200
70_3	1481.12	436.39	1447.99	3365.50	4.87%	7867	1	2.28%	3303.964	1.61%	7200
70_4	1504.29	436.88	1449.31	3390.48	3.93%	7857	1	0.56%	3368.807	1.85%	7200
70_5	1518.24	445.48	1477.91	3441.63	4.50%	7852	1	0.39%	3413.963	2.28%	7200
80_1	1763.12	508.00	1728.19	3999.30	4.16%	8496	1	0.55%	3975.693	2.18%	7200
80_2	1733.11	487.13	1729.51	3949.75	5.13%	13206	1	2.00%	3895.931	2.38%	7200
80_3	1694.05	514.97	1648.20	3857.21	4.50%	8042	1	1.06%	3802.143	1.68%	7200
80_4	1710.63	505.08	1667.45	3883.16	4.30%	7963	1	0.72%	3850.704	2.06%	7200
80_5	1717.45	488.54	1678.71	3884.70	4.23%	7830	1	0.71%	3866.379	2.31%	7200
90_1						7203	1	0.71%	4447.360	2.48%	7200
90_2	1928.17	550.22	1898.94	4377.34	4.30%	8243	1	0.54%	4358.332	2.36%	7200
90_3	1906.16	583.95	1854.56	4344.67	4.51%	8085	1	0.71%	4287.409	1.73%	7200
90_4	1921.81	576.00	1907.73	4405.54	5.02%	8251	1	1.75%	4331.240	1.92%	7200
90_5	1935.16	556.22	1912.22	4403.60	4.50%	8294	1	0.71%	4366.757	2.20%	7200
100_1						7203	1	0.71%	4903.957	2.38%	7200
100_2						7203	1	0.71%	4816.934	2.35%	7200
100_3	2113.94	608.52	2069.56	4792.03	4.06%	8647	1	1.02%	4754.418	1.77%	7200
100_4	2121.79	633.04	2089.49	4844.32	4.42%	8109	1	0.35%	4802.228	2.10%	7200
100_5						7203	1	0.35%	4810.438	2.24%	7200

Table 5.13: Results obtained with the assumption that in the depot there are additional EBs with no routes assigned

	Energy	FRD	Deg	Total	GAP	Time	V2G	V2G %
10_1	263.72	190.85	75.58	530.15	2.82%	3613	0	0
10_2	283.42	206.64	79.76	569.81	1.92%	3607	0	0
10_3	292.76	218.68	80.85	592.29	2.21%	3610	0	0
10_4	281.64	215.98	78.59	576.21	3.40%	3611	0	0
10_5	261.90	184.91	71.98	518.78	2.17%	3613	0	0
20_1	478.86	409.21	139.05	1027.12	3.22%	3644	0	0
20_2	492.10	420.41	139.59	1052.10	2.99%	3650	0	0
20_3	506.55	428.79	143.86	1079.20	2.28%	3628	0	0
20_4	469.99	392.55	133.17	995.71	2.57%	3628	0	0
20_5	466.19	390.90	130.68	987.76	2.96%	3642	0	0
30_1	681.19	607.00	198.72	1486.91	3.00%	3678	0	0
30_2	688.50	618.97	194.56	1502.02	3.23%	3690	0	0
30_3	700.69	618.85	201.17	1520.70	2.37%	3679	0	0
30_4	683.85	605.84	193.23	1482.92	2.76%	3669	0	0
30_5	657.09	573.89	185.54	1416.52	2.57%	3673	0	0
40_1	923.80	851.80	265.37	2040.98	3.03%	3985	0	0
40_2	906.71	837.13	257.27	2001.11	3.29%	3707	0	0
40_3	904.06	820.89	264.04	1988.99	2.55%	3670	0	0
40_4	884.32	803.56	250.83	1938.71	2.74%	3717	0	0
40_5	886.50	815.97	251.46	1953.93	3.26%	3728	0	0
50_1	1124.75	1059.59	326.06	2510.40	3.39%	3774	0	0
50_2	1111.82	1050.36	316.21	2478.38	3.62%	3793	0	0
50_3	1104.29	1014.21	316.13	2434.62	2.44%	3741	0	0
50_4	1104.17	1023.81	314.01	2441.99	2.89%	3794	0	0
50_5	1090.24	1015.20	310.01	2415.45	3.21%	4148	0	0
60_1	1340.17	1278.98	388.28	3007.43	3.51%	3887	0	0
60_2	1326.48	1265.27	377.89	2969.64	3.58%	3981	0	0
60_3	1297.92	1207.34	373.07	2878.34	2.55%	3780	0	0
60_4	1302.27	1223.19	371.79	2897.25	2.98%	3819	0	0
60_5	1297.53	1222.75	369.57	2889.86	3.24%	3860	0	0
70_1	1557.30	1496.00	450.61	3503.91	3.44%	3871	0	0
70_2	1510.96	1451.63	431.62	3394.21	3.72%	3980	0	0
70_3	1480.14	1390.39	422.52	3293.06	2.77%	3848	0	0
70_4	1504.05	1420.17	431.35	3355.57	2.91%	3900	0	0
70_5	1519.03	1449.20	433.22	3401.44	3.36%	3867	0	0
80_1	1762.26	1692.09	507.58	3961.93	3.23%	3883	0	0
80_2	1727.14	1663.94	493.02	3884.09	3.54%	3930	0	0
80_3	1697.28	1609.19	484.85	3791.33	2.87%	3895	0	0
80_4	1711.09	1641.40	490.70	3843.19	3.30%	3959	0	0
80_5	1715.39	1648.76	489.65	3853.80	3.47%	4067	0	0
90_1	1961.68	1909.94	564.67	4436.29	3.66%	3990	0	0
90_2	1926.96	1865.96	550.89	4343.80	3.56%	4023	0	0
90_3	1907.78	1826.08	546.99	4280.85	3.09%	3879	0	0
90_4	1923.92	1836.54	550.19	4310.65	2.93%	4041	0	0
90_5	1934.15	1862.73	552.51	4349.39	3.30%	6390	0	0
100_1	2161.54	2115.23	623.68	4900.45	3.79%	4227	0	0
100_2	2126.55	2101.46	609.81	4837.82	0.00%	535	0	0
100_3	2112.43	2036.79	604.32	4753.54	3.27%	4107	0	0
100_4	2124.92	2057.37	609.32	4791.61	3.35%	4150	0	0
100_5	2127.79	2062.66	608.15	4798.60	3.42%	4189	0	0

Table 5.14: Results obtained with a grid of 30% of the capacity

	Energy	FRD	Deg	Total	GAP	Time	V2G	V2G %
10_1	263.72	190.85	75.58	530.15	2.87%	3613	0.00	0.00
10_2	283.42	206.62	79.76	569.79	1.89%	3610	0.00	0.00
10_3	292.76	218.68	80.85	592.29	2.21%	3608	0.00	0.00
10_4	281.64	215.98	78.59	576.21	3.38%	3614	0.00	0.00
10_5	261.90	184.91	71.98	518.78	2.17%	3609	0.00	0.00
20_1	478.86	409.21	139.05	1027.12	3.19%	3636	0.00	0.00
20_2	492.10	420.41	139.59	1052.10	2.97%	3637	0.00	0.00
20_3	506.55	428.76	143.86	1079.17	2.23%	3630	0.00	0.00
20_4	469.99	392.55	133.17	995.71	2.55%	3631	0.00	0.00
20_5	466.19	390.90	130.68	987.76	2.94%	3645	0.00	0.00
30_1	681.19	607.00	198.72	1486.91	3.01%	3701	0.00	0.00
30_2	688.50	618.97	194.56	1502.02	3.22%	3682	0.00	0.00
30_3	700.69	618.87	201.17	1520.72	2.41%	3657	0.00	0.00
30_4	683.85	605.84	193.23	1482.92	2.80%	3671	0.00	0.00
30_5	657.09	573.93	185.54	1416.55	2.54%	3680	0.00	0.00
40_1	923.80	851.80	265.37	2040.98	3.03%	3706	0.00	0.00
40_2	906.71	837.15	257.27	2001.13	3.30%	3734	0.00	0.00
40_3	904.06	821.17	264.04	1989.27	2.57%	3681	0.00	0.00
40_4	884.32	803.56	250.83	1938.71	2.76%	3722	0.00	0.00
40_5	886.50	815.96	251.46	1953.92	3.24%	3733	0.00	0.00
50_1	1124.75	1060.88	326.06	2511.69	3.44%	3782	0.00	0.00
50_2	1111.82	1046.02	316.21	2474.05	3.45%	3751	0.00	0.00
50_3	1104.29	1014.49	316.13	2434.90	2.45%	3742	0.00	0.00
50_4	1104.17	1025.53	314.01	2443.71	2.97%	3741	0.00	0.00
50_5	1090.24	1016.68	310.01	2416.93	3.28%	3803	0.00	0.00
60_1	1340.17	1281.21	388.28	3009.66	3.58%	3930	0.00	0.00
60_2	1326.48	1264.85	377.89	2969.23	3.57%	3839	0.00	0.00
60_3	1297.92	1208.86	373.07	2879.86	2.59%	3767	0.00	0.00
60_4	1302.23	1223.75	371.97	2897.95	3.03%	3856	0.00	0.00
60_5	1297.53	1224.31	369.57	2891.42	3.30%	3815	0.00	0.00
70_1	1557.30	1494.44	450.61	3502.35	3.38%	3865	0.00	0.00
70_2	1510.96	1455.93	431.62	3398.51	3.85%	5237	0.00	0.00
70_3	1480.14	1390.87	422.52	3293.54	2.79%	3809	0.00	0.00
70_4	1504.05	1419.31	431.35	3354.70	2.90%	3836	0.00	0.00
70_5	1519.03	1463.35	433.22	3415.59	3.73%	5625	0.00	0.00
80_1	1762.26	1692.91	507.58	3962.75	3.24%	3888	0.00	0.00
80_2	1727.14	1663.67	493.02	3883.82	3.52%	4032	0.00	0.00
80_3	1697.24	1606.48	485.04	3788.76	2.78%	4031	0.00	0.00
80_4	1711.05	1633.59	490.89	3835.53	3.10%	4032	0.00	0.00
80_5	1715.39	1650.55	489.65	3855.58	3.51%	3945	0.00	0.00
90_1	1961.68	1910.71	564.67	4437.06	3.69%	4061	0.00	0.00
90_2	1926.92	1873.35	551.07	4351.34	3.71%	3946	0.00	0.00
90_3	1907.76	1834.30	547.08	4289.14	3.27%	3934	0.00	0.00
90_4	1923.96	1836.79	550.00	4310.75	2.92%	4024	0.00	0.00
90_5	1934.15	1881.87	552.51	4368.53	3.72%	4308	0.00	0.00
100_1	2161.54	2116.02	623.68	4901.24	3.79%	4028	0.00	0.00
100_2	2126.55	2092.46	609.81	4828.82	4.09%	5276	0.00	0.00
100_3	2112.49	2027.83	603.76	4744.08	3.10%	4099	0.00	0.00
100_4	2124.92	2052.05	609.32	4786.30	3.24%	4050	0.00	0.00

Table 5.15: Results obtained with a grid of 50% of the capacity

|	Energy	FRD	Deg	Total	GAP	Time	V2G	V2G %
10_1	263.72	75.58	190.85	530.15	2.87%	3613	0	0
10_2	283.42	79.76	206.62	569.79	1.89%	3610	0	0
10_3	292.76	80.85	218.68	592.29	2.21%	3608	0	0
10_4	281.64	78.59	215.98	576.21	3.38%	3614	0	0
10_5	261.90	71.98	184.91	518.78	2.17%	3609	0	0
20_1	478.86	139.05	409.21	1027.12	3.19%	3636	0	0
20_2	492.10	139.59	420.41	1052.10	2.97%	3637	0	0
20_3	506.55	143.86	428.76	1079.17	2.23%	3630	0	0
20_4	469.99	133.17	392.55	995.71	2.55%	3631	0	0
20_5	466.19	130.68	390.90	987.76	2.94%	3645	0	0
30_1	681.19	198.72	607.00	1486.91	3.01%	3701	0	0
30_2	688.50	194.56	618.97	1502.02	3.22%	3682	0	0
30_3	700.69	201.17	618.87	1520.72	2.41%	3657	0	0
30_4	683.85	193.23	605.84	1482.92	2.80%	3671	0	0
30_5	657.09	185.54	573.93	1416.55	2.54%	3680	0	0
40_1	923.80	265.37	851.80	2040.98	3.03%	3706	0	0
40_2	906.71	257.27	837.15	2001.13	3.30%	3734	0	0
40_3	904.06	264.04	821.17	1989.27	2.57%	3681	0	0
40_4	884.32	250.83	803.56	1938.71	2.76%	3722	0	0
40_5	886.50	251.46	815.96	1953.92	3.24%	3733	0	0
50_1	1124.75	326.06	1060.88	2511.69	3.44%	3782	0	0
50_2	1111.82	316.21	1046.02	2474.05	3.45%	3751	0	0
50_3	1104.29	316.13	1014.49	2434.90	2.45%	3742	0	0
50_4	1104.17	314.01	1025.53	2443.71	2.97%	3741	0	0
50_5	1090.24	310.01	1016.68	2416.93	3.28%	3803	0	0
60_1	1340.17	388.28	1281.21	3009.66	3.58%	3930	0	0
60_2	1326.48	377.89	1264.85	2969.23	3.57%	3839	0	0
60_3	1297.92	373.07	1208.86	2879.86	2.59%	3767	0	0
60_4	1302.23	371.97	1223.75	2897.95	3.03%	3856	0	0
60_5	1297.53	369.57	1224.31	2891.42	3.30%	3815	0	0
70_1	1557.30	450.61	1494.44	3502.35	3.38%	3865	0	0
70_2	1510.96	431.62	1455.93	3398.51	3.85%	5237	0	0
70_3	1480.14	422.52	1390.87	3293.54	2.79%	3809	0	0
70_4	1504.05	431.35	1419.31	3354.70	2.90%	3836	0	0
70_5	1519.03	433.22	1463.35	3415.59	3.73%	5625	0	0
80_1	1762.26	507.58	1692.91	3962.75	3.24%	3888	0	0
80_2	1727.14	493.02	1663.67	3883.82	3.52%	4032	0	0
80_3	1697.24	485.04	1606.48	3788.76	2.78%	4031	0	0
80_4	1711.05	490.89	1633.59	3835.53	3.10%	4032	0	0
80_5	1715.39	489.65	1650.55	3855.58	3.51%	3945	0	0
90_1	1961.68	564.67	1910.71	4437.06	3.69%	4061	0	0
90_2	1926.92	551.07	1873.35	4351.34	3.71%	3946	0	0
90_3	1907.76	547.08	1834.30	4289.14	3.27%	3934	0	0
90_4	1923.96	550.00	1836.79	4310.75	2.92%	4024	0	0
90_5	1934.15	552.51	1881.87	4368.53	3.72%	4308	0	0
100_1	2161.54	623.68	2116.02	4901.24	3.79%	4028	0	0
100_2	2126.55	609.81	2092.46	4828.82	4.09%	5276	0	0
100_3	2112.49	603.76	2027.83	4744.08	3.10%	4099	0	0
100_4	2124.92	609.32	2052.05	4786.30	3.24%	4050	0	0
100_5	2127.79	608.15	2055.16	4791.10	3.27%	4032	0	0

Table 5.16: Results obtained with a grid of 70% of the capacity

are employed. In 5.2a there is a panel to show the behavior of a fleet of 10 vehicles in such case.

In general, being more convenient in this case, EBs are charged during the night. Some of them then, discharge energy when they are in the depot during the peak price hours. Notice that the discharged energy is not used to charge other EBs, since none is charging at the same time, but to satisfy the depot demand. This could be an explanation for the poor results obtained in the above situations. It also suggests that V2Gs could be beneficial in grids shared among different buildings. However, the usage of V2Gs is strongly influenced by the context and in particular the other costs. Indeed, the same instance optimized according to all the costs (5.2b), produces a schedule that does not exploit V2Gs.
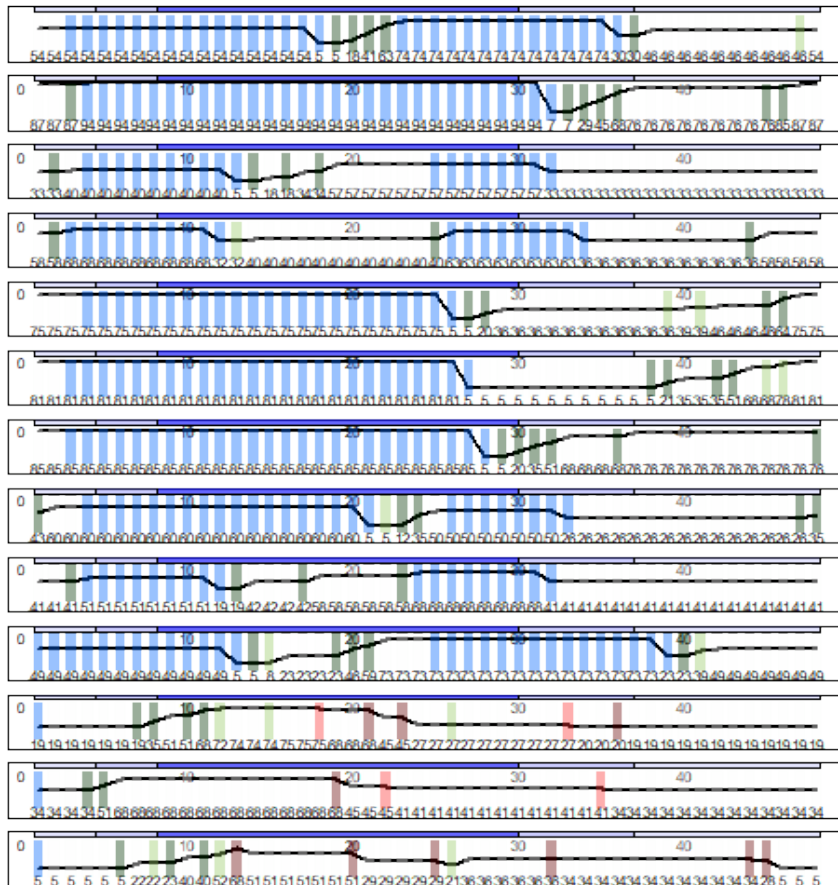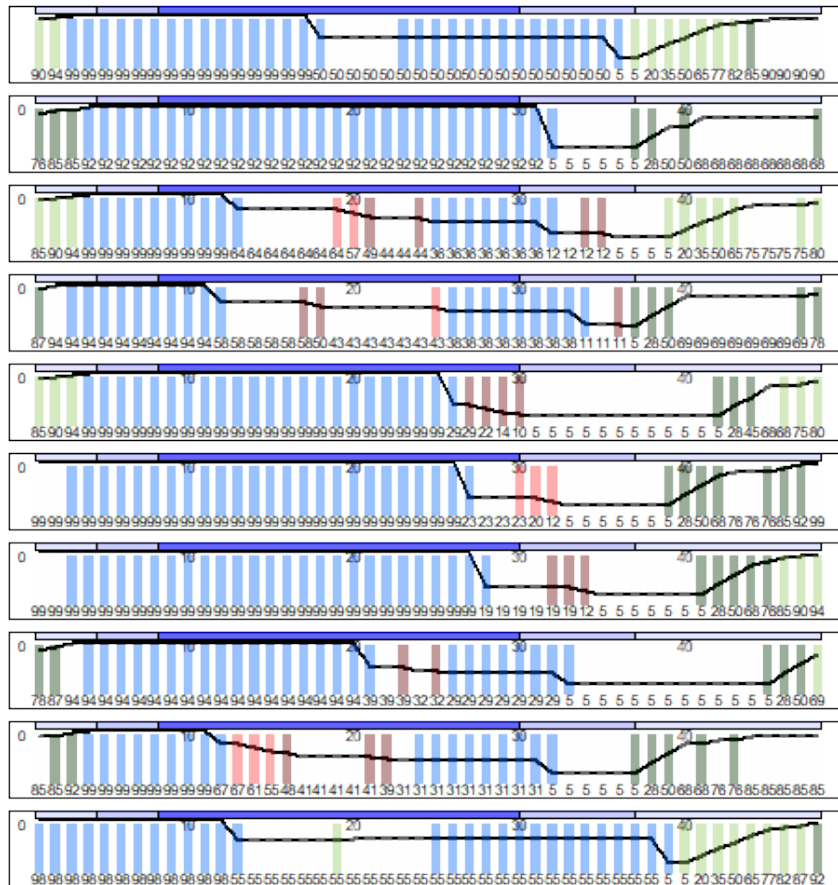
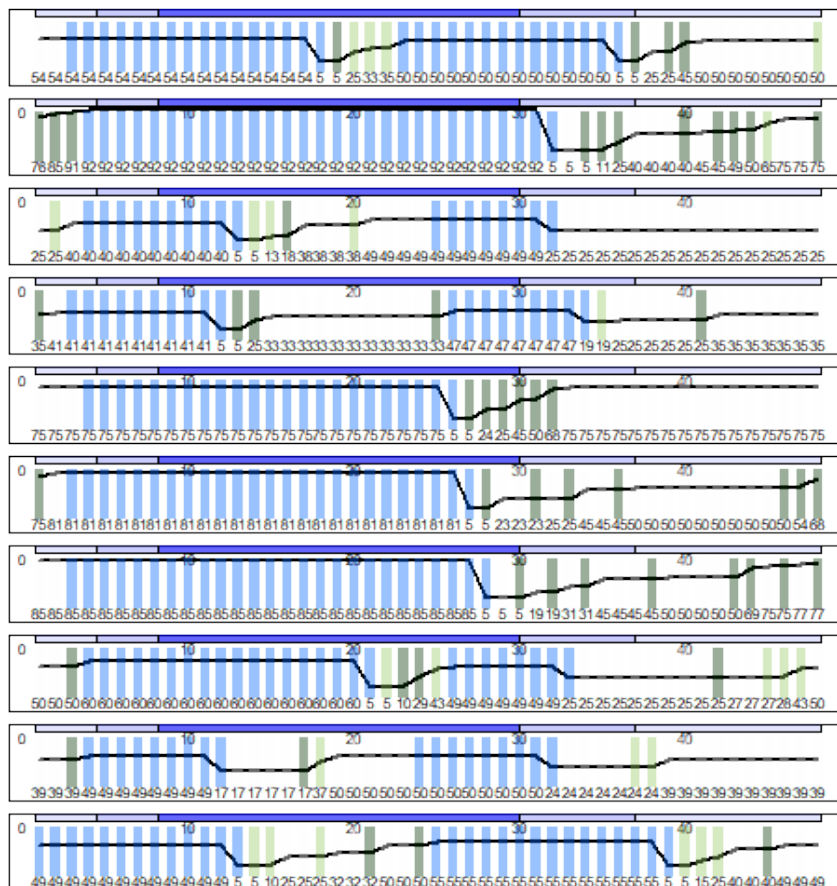**(a)** Charging plan for the fleet when only energy costs are optimized
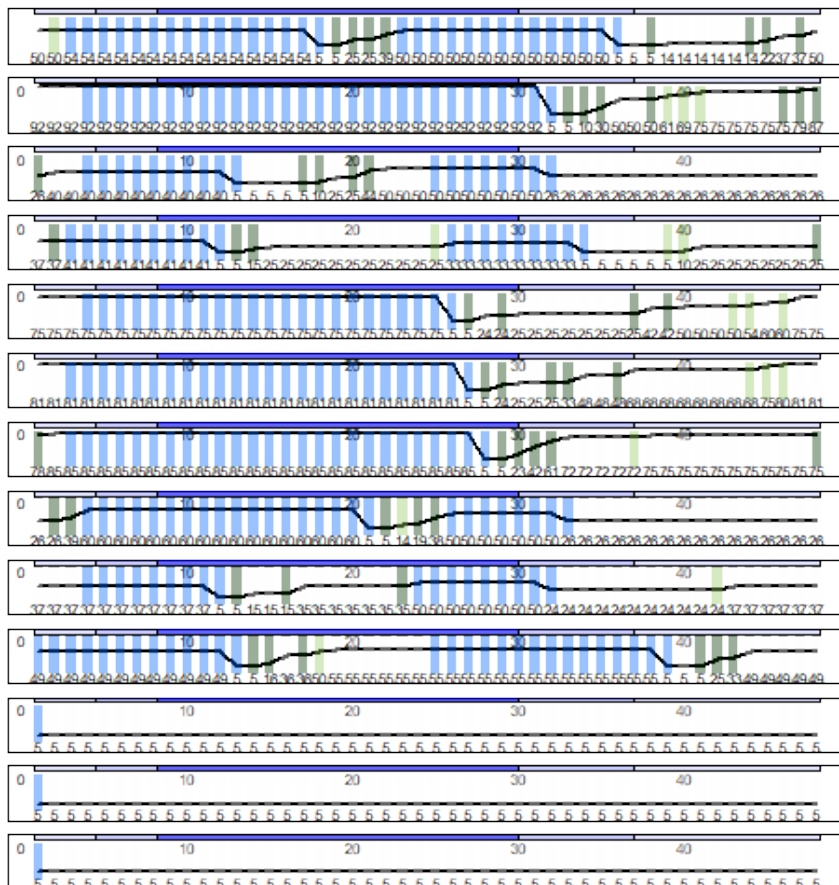
(b) Charging plan for the fleet according to the full model

Figure 5.1: The two step solution obtained for the instance 10_1 considering extre vehicles

(a) Charging plan of the fleet with extra EBs when degradation costs are not considered

(b) Charging plan of the fleet with extra EBs

Figure 5.2: Comparison of two charge scheduling for the same fleet

Chapter 6

Conclusions

An optimization model has been implemented to optimize the charging scheduling of an electric fleet of buses provided with Vehicle-to-Grid technologies. The objective of this scheduling is to develop a charge routing for the fleet which allows all the buses to perform their routes. At the same time, it helps in keeping at their lowest all the costs, such as the one for withdrawing electricity from the grid, facility-related demand charges for the maximum charging power required and degradation costs related to battery usage.

Particular attention has been devoted to the integration of V2G technologies in the model. The revenue of the grid when adopting V2Gs has been computed and, accordingly, the power requested to the grid in every period modified. A contribution for the energy has been modelled too. Finally, also the degradation costs are extended to the setting pf bidirectional current, considering a theoretical framework to convert the usage into monetary costs.

A public transportation system setting has been recreated for the case study. Data and instances have been investigated and simulated on the base of Milan public transportation system. The model has proved to be inefficient in this setting, as no solution are found within time limit if the fleets are above 30 units. For this reason, sub-models of the original one have been solved analyzing their complexity. On the base of the results, a two stage optimization strategy has been developed to solve the problem. By means of this strategy, managerial insights are performed to investigate whether V2G technologies are adopted and if the goodness of the solution improves.

In most of the analyzed situation, V2G technologies are not beneficial, mainly because they tend to increase the degradation costs and require higher power. Indeed, we have seen that even if V2Gs are used when we optimize only the energy or energy and FRD, once we introduce the degradation costs, these technologies are no longer exploited. Furthermore, their usage is strictly related to the setting and adding more flexibility can lead to better results. In particular, spare vehicles without assigned routes contribute to the energy profile of the depot charging energy in low cost periods and discharging during the high ones. Finally we have shown how V2G technologies are exploited when energy costs are optimized. They are used to store energy bought at cheap price and use it in high cost period. Providing partially a fleet with V2G technologies can therefore be beneficial. Furthermore, V2G technologies can be also beneficial for ancillary services that in this particular

context are ignored. An analysis in such scenario could lead even to better results. Lastly, the matheuristic developed relies on the fast resolution of particular sub problems. This strongly depend on the choice of the parameters of the problem. The development of a constructive heuristic could extend the applicability of the model in wider contexts.

Appendix A

Appendix: Table of notation

$\mathcal{P}$	Set of periods in the planning interval
n_p	Number of periods in $\mathcal{P}$
δ	Length of each period in hours
π_p	Demand of the depot in every period p $\forall p \in \mathcal{P}$
$\mathcal{K}$	Set of EVs
m	Number of EVs in $\mathcal{K}$
Q	Battery charge capacity (Ah)
E	Battery energy capacity (kWh)
f_k	Earliest route of vehicle k $\forall k \in \mathcal{K}$
l_k	Latest route of vehicle k $\forall k \in \mathcal{K}$
$\mathcal{R}$	Set of routes
ΔSOC_r	Charge consumption of route r $\forall r \in \mathcal{R}$
η_r	Route of vehicle k_r with the latest arrival period prior to β_r $\forall r \in \mathcal{R}$
β_r	Departure period of route r $\forall r \in \mathcal{R}$
α_r	Arrival period of route r $\forall r \in \mathcal{R}$
k_r	Vehicle that must perform route r $\forall r \in \mathcal{R}$
$\mathcal{S}$	Set of types of chargers installed at the depot
B_s	Set of breakpoints used in the piecewise linear approximation of the CC-CV charging function of charger type s $\forall s \in \mathcal{S}$
κ_s	Number of chargers of type s installed at the depot $\forall s \in \mathcal{S}$
a_{si}	SOC associated with breakpoint $i \in B_s$ of the piecewise linear approximation of the CC-CV charging function of charger type s $s \in \mathcal{S}, \forall i \in B_s \setminus \{0\}$
I_{si}	Charging current (A) used in the piecewise linear approximation of the CC-CV charging function of charger type s between breakpoints i and $i-1$, with $i \in B_s \setminus \{0\}$, $\forall s \in \mathcal{S}, \forall i \in B_s \setminus \{0\}$
C	Maximum number of charging events between each arrival and departure for each vehicle
$\mathcal{D}$	Number of breakpoints in the wear cost function
L	Length of each interval of the SOC

$\bar{\delta}_d$	Upper bound in the d-th interval of the SOC $\forall d \in \mathcal{D}$
w_d	Value of the wear cost function evaluated at d SOC $\forall d \in \mathcal{D}$
c_p	Energy cost during period p $\forall p \in \mathcal{P}$ ($/kWh)
F	FRD charge ($/kW)
G	Grid restriction (kW)

Table A.1: Complete list of parameters

SOC_{pk}	Decision variable indicating the SOC of vehicle k at the start of period p $\forall p \in \mathcal{P}, k \in \mathcal{K}$
i_{pk}	Decision variable indicating the charging current (A) applied to vehicle k during period p $\forall p \in \mathcal{P}, k \in \mathcal{K}$
x_{pksi}	Binary decision variable worth 1 if vehicle k uses a charger of type s along the segment i of the piece-wise linear approximation during period p with SOC values at the start and end of p $\forall p \in \mathcal{P}, k \in \mathcal{K}, s \in \mathcal{S}, i \in B_s \setminus \{0\}$ used in the non V2G settings
x^+_{pksi}	Binary decision variable worth 1 if vehicle k charges using a charger of type s along the segment i of the piece-wise linear approximation during period p with SOC values at the start and end of p $\forall p \in \mathcal{P}, k \in \mathcal{K}, s \in \mathcal{S}, i \in B_s \setminus \{0\}$
x^-_{pksi}	Binary decision variable worth 1 if vehicle k discharges using a charger of type s along the segment i of the piece-wise linear approximation during period p with SOC values at the start and end of p $\forall p \in \mathcal{P}, k \in \mathcal{K}, s \in \mathcal{S}, i \in B_s \setminus \{0\}$
Φ_{pksi}	Quantity of SOC charged in vehicle k at period p using the charger s along the segment i of the piece-wise linear approximation of the CC-CV curve $\forall p \in \mathcal{P}, k \in \mathcal{K}, s \in \mathcal{S}, i \in B_s \setminus \{0\}$ used in the non V2G settings
Φ^+_{pksi}	Quantity of SOC charged in vehicle k at period p using the charger s along the segment i of the piece-wise linear approximation of the CC-CV curve $\forall p \in \mathcal{P}, k \in \mathcal{K}, s \in \mathcal{S}, i \in B_s \setminus \{0\}$
Φ^-_{pksi}	Quantity of SOC discharged in vehicle k at period p using the charger s along the segment i of the piece-wise linear approximation of the CC-CV curve $\forall p \in \mathcal{P}, k \in \mathcal{K}, s \in \mathcal{S}, i \in B_s \setminus \{0\}$
q_{pks}	Binary variable that control whether vehicle k is being charged during period p with charger s $\forall p \in \mathcal{P}, k \in \mathcal{K}, s \in \mathcal{S}$ used in the non V2G settings
q^+_{pks}	Binary variable that control whether vehicle k is being charged during period p with charger s $\forall p \in \mathcal{P}, k \in \mathcal{K}, s \in \mathcal{S}$
q^-_{pks}	Binary variable that control whether vehicle k is being discharged during period p with charger s $\forall p \in \mathcal{P}, k \in \mathcal{K}, s \in \mathcal{S}$
y	Decision variable indicating the maximum charging power (kW) retrieved from the grid during the planning interval

z_{pk}	Binary decision variable worth 1 if a charging event occurs for vehicle k at time p during period p $\forall p \in \mathcal{P}, k \in \mathcal{K}, s \in \mathcal{S}, i \in B_s \setminus \{0\}$
soc_{dr}^+	Quantity of SOC charged before route r in vehicle k_r along segment d $\forall r \in \mathcal{R}, d \in \mathcal{D}$ used in the non V2G settings
soc_{pdk}^+	Percentage of energy charged at period p by vehicle k along segment d $\forall p \in \mathcal{P}, d \in \mathcal{D}, k \in \mathcal{K}$
u_{dr}^+	Binary variable that indicates whether some SOC is charged before route r in vehicle k_r along segment d $\forall r \in \mathcal{R}, d \in \mathcal{D}$ used in the non V2G settings
u_{pdk}^+	Binary variable that indicates whether some SOC is charged at period p by vehicle k along segment d $\forall p \in \mathcal{P}, d \in \mathcal{D}, k \in \mathcal{K}$

Table A.2: Complete list of variables

Acronyms

EV   Electric Vehicle

V2G   Vehicle-to-Grid

EV-V2G   Electric Vehicle provided with Vehicle-to-Grid technologies

EB   Electric Bus

FRD   Facility Related Demand

EV-CSP   Electric Vehicles Charge Scheduling Problem

EEV-CSP   Enhanced Electric Vehicles Charge Scheduling Problem

EEV-CSP-V2G   Enhanced Electric Vehicles Charge Scheduling Problem with Vehicle-to-Grid technologies

Bibliography

Abdelwahed, Ayman, Pieter L van den Berg, Tobias Brandt, John Collins, and
      Wolfgang Ketter
    2020   "Evaluating and optimizing opportunity fast-charging schedules in
         transit battery electric bus networks", *Transportation Science*, 54, 6,
         pp. 1601-1615. (Cit. on p. 5.)

Abdulaal, Ahmed, Mehmet H Cintuglu, Shihab Asfour, and Osama A Mohammed
    2016   "Solving the multivariant EV routing problem incorporating V2G and
         G2V options", *IEEE Transactions on Transportation Electrification*,
         3, 1, pp. 238-248.

Alvo, Matıas, Gustavo Angulo, and Mathias Klapp
    2021   "An exact solution approach for an electric bus dispatch problem".
         (Cit. on pp. 6, 7.)

An, Kun
    2020   "Battery electric bus infrastructure planning under demand uncer-
         tainty", *Transportation Research Part C: Emerging Technologies*, 111,
         pp. 572-587. (Cit. on p. 5.)

Arif, AI, M Babar, TP Imthias Ahamed, EA Al-Ammar, PH Nguyen, IG René
      Kamphuis, and NH Malik
    2016   "Online scheduling of plug-in vehicles in dynamic pricing schemes",
         Sustainable Energy, Grids and Networks, 7, pp. 25-36.

ATMWebsite
    n.d.   *ATM: DAL 2030 FULL ELECTRIC*, https://www.atm.it/it/AtmN
         ews/Comunicati/Pagine/ATMDAL2030FULLELECTRIC.aspx. (Cit. on
         pp. 2, 33.)

Brito, Martins, Pedrosa, Monteiro, and Afonso
    2013   "Real-life comparison between diesel and electric car energy consump-
         tion". (Cit. on p. 2.)

Dai, Qian, Tao Cai, Shanxu Duan, and Feng Zhao
    2014   "Stochastic modeling and forecasting of load demand for electric bus
         battery-swap station", *IEEE Transactions on Power Delivery*, 29, 4,
         pp. 1909-1917.

DeForest, Nicholas, Jason S MacDonald, and Douglas R Black

    2018   "Day ahead optimization of an electric vehicle fleet providing ancillary services in the Los Angeles Air Force Base vehicle-to-grid demonstration", *Applied energy*, 210, pp. 987-1001.

Deng, Ruilong, Yuan Liu, Wenzhuo Chen, and Hao Liang

    2019   "A Survey on Electric Buses—Energy Storage, Power Management, and Charging Scheduling", *IEEE Transactions on Intelligent Transportation Systems*, 22, 1, pp. 9-22. (Cit. on p. 5.)

Di Milano, Comune

    2021   https://dati.comune.milano.it/dataset/ds534-atm-fermate-linee-di-superficie-urbane.

  n.d.(a) *open data Comune di Milano*, https://dati.comune.milano.it/dataset/ds536_atm-orari-linee-di-superficie-urbane. (Cit. on p. 35.)

  n.d.(b) *open data Comune di Milano (1)*, https://dati.comune.milano.it/dataset/ds538_atm-percorsi-linee-di-superficie-urbane. (Cit. on p. 35.)

EEA

    2020a *Air quality in Europe - 2020 report*, tech. rep., EEA. (Cit. on p. 1.)

    2020b *Measures to reduce emissions of air pollutants and greenhouse gases: the potential for synergies*, tech. rep., EEA. (Cit. on p. 1.)

    2020c *Use of renewable energy for transport in Europe*, tech. rep., EEA. (Cit. on p. 1.)

    2021 *EEA Signals 2020: Towards zero pollution in Europe*, tech. rep., EEA. (Cit. on p. 1.)

EEA, EE

    2019 *Greenhouse gas emissions from transport in Europe*. (Cit. on p. 1.)

Elmehdi, Mabrouk and Maach Abdelilah

    2019 "Genetic algorithm for optimal charge scheduling of electric vehicle fleet", in *Proceedings of the 2nd International Conference on Networking, Information Systems & Security*, pp. 1-7.

Erdelić, Tomislav and Tonči Carić

    2019 "A survey on the electric vehicle routing problem: variants and solution approaches", *Journal of Advanced Transportation*, 2019. (Cit. on p. 5.)

Farzin, Hossein, Mahmud Fotuhi-Firuzabad, and Moein Moeini-Aghtaie

    2016 "A practical scheme to involve degradation cost of lithium-ion batteries in vehicle-to-grid applications", *ieee transactions on sustainable energy*, 7, pp. 1730-1738. (Cit. on p. 12.)

Finance, Bloomberg New Energy

    2020 *New Energy Outlook 2020*, tech. rep., Technical report. (Cit. on pp. 1, 33, 47.)

Froger, Aurélien, Jorge E Mendoza, Ola Jabali, and Gilbert Laporte

    2019   "Improved formulations and algorithmic components for the electric vehicle routing problem with nonlinear charging functions", *Computers & Operations Research*, 104, pp. 256-294. (Cit. on p. 15.)

Han, Han, and Aki

    2014   "A practical battery wear model for electric vehicle charging applications", *Applied Energy*, 113, pp. 1100-1108. (Cit. on pp. 9, 12-14, 26.)

Han, Sekyung, Hirohisa Aki, and Soohee Han

    2012   "Optimal charging strategy of a PEV battery considering frequency regulation and distributed generation", in *2012 IEEE Vehicle Power and Propulsion Conference*, IEEE, pp. 1014-1019. (Cit. on p. 26.)

Iacobucci, Riccardo, Benjamin McLellan, and Tetsuo Tezuka

    2019   "Optimization of shared autonomous electric vehicles operations with charge scheduling and vehicle-to-grid", *Transportation Research Part C: Emerging Technologies*, 100, pp. 34-52.

Jang, Young Jae, Eun Suk Suh, and Jong Woo Kim

    2015   "System architecture and mathematical models of electric transit bus system utilizing wireless power transfer technology", *IEEE Systems Journal*, 10, 2, pp. 495-506. (Cit. on p. 6.)

Janovec and Koháni

    2019   "Exact approach to the electric bus fleet scheduling", *Transportation Research Procedia*, 40, pp. 1380-1387. (Cit. on pp. 6, 7.)

Kempton, Willett and Jasna Tomić

    2005   "Vehicle-to-grid power fundamentals: Calculating capacity and net revenue", *Journal of power sources*. (Cit. on pp. 23, 24.)

Larminie, James and John Lowry

    2012   *Electric vehicle technology explained*, John Wiley & Sons. (Cit. on pp. 9, 10.)

Montoya, Alejandro, Christelle Guéret, Jorge E Mendoza, and Juan G Villegas

    2017   "The electric vehicle routing problem with nonlinear charging function", *Transportation Research Part B: Methodological*, 103, pp. 87-110.

Ning, Gang, Ralph E White, and Branko N Popov

    2006   "A generalized cycle life model of rechargeable Li-ion batteries", *Electrochimica acta*, 51, pp. 2012-2022. (Cit. on p. 12.)

Pelletier, Jabali, and Laporte

    2018   "Charge scheduling for electric freight vehicles", *Elsevier*. (Cit. on pp. 2, 6, 7, 9, 11, 16, 18, 20, 21, 24.)

Pelletier, Samuel, Ola Jabali, Gilbert Laporte, and Marco Veneroni

2017   "Battery degradation and behaviour for electric vehicles: Review and numerical analyses of several models", *Transportation Research Part B: Methodological*. (Cit. on p. 12.)

Pelletier, Samuel, Ola Jabali, Jorge E Mendoza, and Gilbert Laporte

2019   "The electric bus fleet transition problem", *Transportation Research Part C: Emerging Technologies*. (Cit. on pp. 5, 33.)

ROSSETTI, FEDERICA

2020   "Optimization model for charge scheduling of electric freight vehicles: the Italian case". (Cit. on p. 33.)

Schmidt, Oliver, Adam Hawkes, Ajay Gambhir, and Iain Staffell

2017   "The future cost of electrical energy storage based on experience rates", *Nature Energy*, 2, 8, pp. 1-8. (Cit. on p. 1.)

Shen, Zuo-Jun Max, Bo Feng, Chao Mao, and Lun Ran

2019   "Optimization models for electric vehicle service operations: A literature review", *Transportation Research Part B: Methodological*, 128, pp. 462-477. (Cit. on p. 5.)

Shepherd, Clarence M

1965   "Design of primary and secondary cells: II. An equation describing battery discharge", *Journal of the Electrochemical Society*. (Cit. on pp. 10, 11.)

Sortomme, Eric and Mohamed A El-Sharkawi

2010   "Optimal charging strategies for unidirectional vehicle-to-grid", *IEEE Transactions on Smart Grid*, 2, 1, pp. 131-138. (Cit. on p. 5.)

Sovacool, Benjamin K, Lance Noel, Jonn Axsen, and Willett Kempton

2018   "The neglected social dimensions to a vehicle-to-grid (V2G) transition: a critical and systematic review", *Environmental Research Letters*, 13, 1, p. 013001. (Cit. on p. 5.)

Spitzer, Martin, Jonas Schlund, Elpiniki Apostolaki-Iosifidou, and Marco Pruckner

2019   "Optimized integration of electric vehicles in low voltage distribution grids", *Energies*, 12, 21, p. 4059. (Cit. on pp. 6, 7.)

Tang, Wanrong, Suzhi Bi, Ying Jun Zhang, and Xiaojun Yuan

2017   "Joint routing and charging scheduling optimizations for smart-grid enabled electric vehicle networks", in *2017 IEEE 85th Vehicular Technology Conference (VTC Spring)*, IEEE, pp. 1-5. (Cit. on p. 5.)

Teixeira, Ana Carolina Rodrigues and José Ricardo Sodré

2018   "Impacts of replacement of engine powered vehicles by electric vehicles on energy consumption and CO2 emissions", *Transportation Research Part D: Transport and Environment*, 59, pp. 375-384. (Cit. on p. 1.)

Tremblay, Olivier, Louis-A Dessaint, and Abdel-Illah Dekkiche

2007   "A generic battery model for the dynamic simulation of hybrid electric vehicles", in *2007 IEEE Vehicle Power and Propulsion Conference*, Ieee, pp. 284-289. (Cit. on pp. 7, 10, 11, 24.)

Triviño-Cabrera, Alicia, José A Aguado, and Sebastián de la Torre

2019   "Joint routing and scheduling for electric vehicles in smart grids with V2G", *Energy*, 175, pp. 113-122. (Cit. on p. 5.)

Vayá, Marina González and Göran Andersson

2014   "Optimal bidding strategy of a plug-in electric vehicle aggregator in day-ahead electricity markets under uncertainty", *IEEE transactions on power systems*, 30, 5, pp. 2375-2385.

Wang, Xiumin, Chau Yuen, Naveed Ul Hassan, Ning An, and Weiwei Wu

2016   "Electric vehicle charging station placement for urban public bus systems", *IEEE Transactions on Intelligent Transportation Systems*, 18, 1, pp. 128-139.

Wang, Yusheng, Yongxi Huang, Jiuping Xu, and Nicole Barclay

2017   "Optimal recharging scheduling for urban electric buses: A case study in Davis", *Transportation Research Part E: Logistics and Transportation Review*, 100, pp. 115-132. (Cit. on p. 5.)

Wen, Min, Esben Linde, Stefan Ropke, P Mirchandani, and Allan Larsen

2016   "An adaptive large neighborhood search heuristic for the electric vehicle scheduling problem", *Computers & Operations Research*, 76, pp. 73-83. (Cit. on pp. 6, 7.)

Yang, Chao, Wei Lou, Junmei Yao, and Shengli Xie

2017   "On charging scheduling optimization for a wirelessly charged electric bus system", *IEEE Transactions on Intelligent Transportation Systems*, 19, 6, pp. 1814-1826. (Cit. on p. 6.)

Yao, Enjian, Tong Liu, Tianwei Lu, and Yang Yang

2020   "Optimization of electric vehicle scheduling with multiple vehicle types in public transport", *Sustainable Cities and Society*, 52, p. 101862. (Cit. on pp. 6, 7.)

Yıldırım, Şule and Barış Yıldız

2021   "Electric bus fleet composition and scheduling", *Transportation Research Part C: Emerging Technologies*, 129, p. 103197. (Cit. on p. 5.)

Zhang, Yiling, Mengshi Lu, and Siqian Shen

2021   "On the values of vehicle-to-grid electricity selling in electric vehicle sharing", *Manufacturing & Service Operations Management*, 23, 2, pp. 488-507. (Cit. on p. 5.)

Zhou, Guang-Jing, Dong-Fan Xie, Xiao-Mei Zhao, and Chaoru Lu

    2020   "Collaborative Optimization of Vehicle and Charging Scheduling for a Bus Fleet Mixed With Electric and Traditional Buses", *IEEE Access*, 8, pp. 8056-8072. (Cit. on p. 5.)

Ziemann, Saskia, Daniel B Müller, Liselotte Schebek, and Marcel Weil

    2018   "Modeling the potential impact of lithium recycling from EV batteries on lithium demand: a dynamic MFA approach", *Resources, conservation and recycling*, 133, pp. 76-85. (Cit. on p. 2.)